# A Probabilistic Framework for Temporal Distribution Generalization in Industry-Scale Recommender Systems

Yuxuan Zhu iamyuxuanzhu@gmail.com Shopee Pte. Ltd. Shanghai, China Cong Fu fc731097343@gmail.com Shopee Pte. Ltd. Singapore Yabo Ni Nanyang Technological University Singapore, Singapore yabo001@e.ntu.edu.sg

# Anxiang Zeng

Nanyang Technological University Singapore, Singapore zeng0118@e.ntu.edu.sg

## **Abstract**

Temporal distribution shift (TDS) erodes the long-term accuracy of recommender systems, yet industrial practice still relies on periodic incremental training, which struggles to capture both stable and transient patterns. Existing approaches such as invariant learning and self-supervised learning offer partial solutions but often suffer from unstable temporal generalization, representation collapse, or inefficient data utilization. To address these limitations, we propose ELBO<sub>TDS</sub>, a probabilistic framework that integrates seamlessly into industry-scale incremental learning pipelines. First, we identify key shifting factors through statistical analysis of real-world production data and design a simple yet effective data augmentation strategy that resamples these time-varying factors to extend the training support. Second, to harness the benefits of this extended distribution while preventing representation collapse, we model the temporal recommendation scenario using a causal graph and derive a selfsupervised variational objective, ELBO<sub>TDS</sub>, grounded in the causal structure. Extensive experiments supported by both theoretical and empirical analysis demonstrate that our method achieves superior temporal generalization, yielding a 2.33% uplift in GMV per user and has been successfully deployed in Shopee Product Search. Code is available at https://github.com/FuCongResearchSquad/ELBO4TDS.

## **CCS** Concepts

- $\bullet \ Computing \ methodologies \rightarrow Multi-task \ learning; \ Ranking;$
- Applied computing  $\rightarrow$  Electronic commerce; Information systems  $\rightarrow$  Information retrieval.

# Keywords

Distribution Shift, Recommender System, Self-Supervised Learning

# 1 Introduction

Modern recommender systems extensively leverage historical interactions such as clicks and purchases in e-commercial recommender to model user preferences [13, 38, 55, 68]. However, most of the common practices leverage empirical risk minimization (ERM) to train the model, implicitly assuming historical and future interactions are independent and identically distributed (IID), which is typically violated in real-world scenarios. User behavior evolves

# Yuan Fang Singapore Management University Singapore, Singapore

yfang@smu.edu.sg

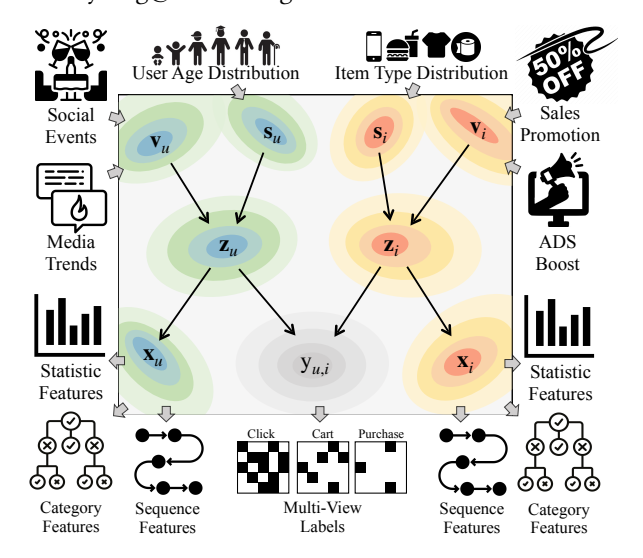


Figure 1: Causal graph representing the data generation process under the temporal distribution shift perspective. Subscript u and i indicate user-specific and item-specific variables, respectively. v denotes time-varying factors, s denotes relatively stable factors, z denotes latent variables (representations), x denotes observed samples, and y denotes labels. Black arrows indicate directions of causal dependencies.

rapidly due to both internal interventions (e.g., flash sales, marketing campaigns) and external shocks (e.g., media influence, seasonality). These evolving patterns lead to temporal distribution shift (TDS)—a fundamental yet under-addressed problem that degrades model performance over time.

A common industrial workaround is periodic incremental training, where models are fine-tuned on newly collected data (e.g., hourly or daily) rather than relying on a fixed checkpoint. While this approach helps capture emerging patterns, it also introduces instability. Models trained under rapidly shifting dynamics may fail to retain long-term preference signals, leading to noisy updates and brittle generalization. Although TDS has attracted limited attention in prior work, two promising paradigms offer partial remedies:

1. Invariant Learning [1, 29, 32, 46]: These methods attempt to eliminate spurious correlations across environments: typically defined by domain, task, or in our case, time windows. However, these methods face two practical limitations in recommendation: (i) Defining environments is non-trivial: TDS varies continuously, and fixed time-window segmentation often fails to capture meaningful shifts. (ii) High storage and training overhead: Invariant learning relies on accessing and mixing historical data, which is costly and delays updates in incremental industry-scale systems.

2. Self-Supervised Learning (SSL) with Data Augmentation [48, 62]: These methods generate augmented views of input samples to expand the support of the training distribution, improving generalization. When applied to TDS, augmentation which simulates realistic time shifts can help to remove time-varying noises. However, discriminative SSL methods such as InfoNCE [53] typically pull augmented views of the same semantics toward the original, suppressing variations. While this encourages temporal stability, our analysis (Section 3.4) shows that it also risks eliminating essential personalized signals, thereby reducing recommendation quality.

To address these limitations, we resort to a generative modeling perspective [22, 42] to shed light on the recommendation under TDS. Specifically, we propose ELBO<sub>TDS</sub>, a probabilistic framework that embeds a data augmentation strategy into a causal variational objective to improve robustness and personalization.

We begin by constructing a causal graph (Figure 1) that explicitly models how time-invariant factors  $\mathbf{s}$  and time-varying factors  $\mathbf{v}$  influence both features  $\mathbf{x}$  and labels y via a latent variable  $\mathbf{z}$ .

Our objective is to factor out  $\mathbf{v}$  while preserving  $\mathbf{s}$ . To achieve this, we inject controlled time-varying perturbations into training samples—guided by statistical insights from real production data, and formulate an Evidence Lower Bound (ELBO) objective that: (i) Filters out time-dependent noise by aligning the latent  $\mathbf{z}$  of augmented views with the original; (2) Preserves both distinctive characteristics (of users and items) and predictive signals by jointly modeling  $\mathbf{z} \to \mathbf{x}$  and  $\mathbf{z} \to \mathbf{y}$ .

Our augmentation strategy is designed with industry constraints in mind. Based on empirical analyses of real-world feature drifts, we introduce lightweight, feature-type-specific transformations (categorical, statistical, sequential) to simulate plausible temporal variations. These augmentations extend the training distribution and improve model robustness without additional online latency or storage cost.

ELBO<sub>TDS</sub> is modular and can be plugged into existing architectures, such as multitask learning [36, 39, 51, 56], sequential models [16, 25, 49], and list-wise ranking [4, 57], with minor changes.

Our main contributions are summarized as follows: (1) A Unified Probabilistic Framework for TDS: We present ELBO<sub>TDS</sub>, a novel generative objective derived from a causal graph, designed to counteract temporal distribution shifts in large-scale recommender systems. (2) Robust Industrial Integration: We introduce a simple yet effective augmentation strategy tailored to real-world feature dynamics. Our method improves GMV/user by 2.33% in online A/B tests and is fully deployed in Shopee Search, a leading e-commerce platform in Southeast Asia. (3) Benchmark Dataset: To encourage further research on TDS, we release a large-scale

industry dataset with hundreds of millions of samples and over 200 engineered features, capturing real-world temporal dynamics.

#### 2 Problem Definition

We consider the challenge of recommendation under TDS, where both user and item variables evolve over time due to various factors. Let  $\mathcal{U}$  and  $\mathcal{I}$  denote the sets of users and items, respectively. At any time span t (e.g., a natural day or hour), we observe a dataset  $\mathcal{D}_t = \{(x_{u,i,t}, y_{u,i,t})\}$ , where  $x_{u,i,t}$  denotes an observed sample (a feature set) for user u and item i at t, and  $y_{u,i,t}$  is the interaction label (e.g., click, purchase) associated with (u,i) during t.

The temporal nature of the problem imposes the following constraints. (1) **Periodic Training**: The model is trained periodically on a sequence of datasets  $\{\mathcal{D}_t\}_{t\leq T}$ , which are collected up to a current time span T. (2) **Future Prediction**: After training, the model is deployed to predict user behavior for the next time span T+1. Importantly, data from T+1 remains **unavailable for training** and can only be accessed once the time window T+1 ends.

# 3 Probabilistic Framework ELBO<sub>TDS</sub>

In this section, we present a probabilistic framework to address temporal distribution shift (TDS) while preserving critical information for downstream recommendation tasks. We begin by analyzing feature shifts over time in large-scale industrial recommender systems, from which we formulate a key hypothesis that guides the design of our method. Building on this insight, we construct a causal graph to disentangle time-invariant and time-varying factors, and derive the ELBO<sub>TDS</sub> objective. This objective is tightly coupled with a data augmentation strategy tailored to the observed temporal dynamics. Finally, we revisit InfoNCE from a probabilistic perspective, revealing its tendency toward representation collapse and discussing its limitations for downstream discriminative tasks under distributional shift.

### 3.1 Empirical Observation of TDS

Modern industrial recommender systems rely heavily on sophisticated feature engineering to improve recommendation quality. However, effectively filtering out time-varying noise, especially the kind that is irrelevant to downstream tasks, requires a deep understanding of how features evolve in real-world production environments. To this end, we conduct a comprehensive empirical study on Shopee's main scenario, analyzing temporal distribution shifts across three widely used feature types: statistical, sequential, and categorical features (see Appendix B.7 for further details).

Our analysis reveals that different feature types exhibit distinct patterns of temporal variation. To systematically quantify these shifts, we adopt two key metrics: the Coefficient of Variation (CV), which measures the relative variability of a feature with respect to its mean, and the Jensen–Shannon Divergence (JSD), which quantifies the distributional divergence between two temporal snapshots. The results, visualized in Figure 2, yield three core insights: (1) All features fluctuate over time, but the degree of variation differs significantly; (2) For most items and users, these fluctuations remain bounded. For example, the 3-day mean click-through rate (CTR) of most items exhibits a CV less than 4, suggesting "stable" short-term dynamics. (3) While short-term variations are prominent, they do

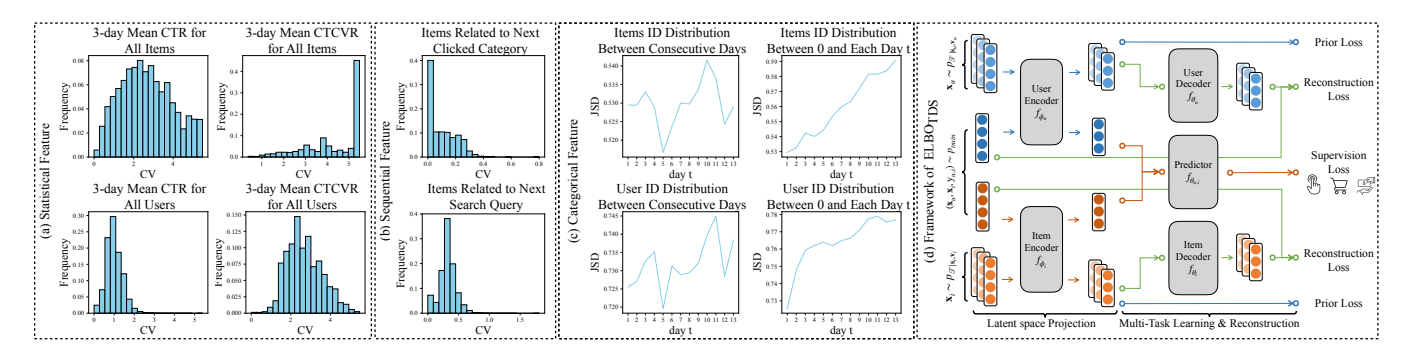


Figure 2: The statistical analysis of the distribution shift for statistical (a), sequential (b), and categorical (c) features, showing significant fluctuations and contributing to the sample TDS. Right side (d) illustrates the architecture of ELBO $_{\rm TDS}$ .

not accumulate significantly over time. This is evidenced by JSD values in Figure 2(c), where the divergence between day 0 and day 13 is only marginally higher than that between day 0 and day 1.

These empirical observations motivate the following hypothesis on TDS in recommender, which underpins our method design:

Hypothesis 1 (Stable-Drifting Distribution Hypothesis). Within a manageable time window, user preferences and item performance are governed by stable latent factors s. Meanwhile, separable time-varying factors v cause short-term fluctuations in the observed data distribution, resulting in variations around a stable distributional core.

#### 3.2 Derivation of ELBO<sub>TDS</sub>

Building on Hypothesis 1, we revisit the data generation process and introduce a corresponding optimization framework.

First, we present a unified data-generation process (Figure 1) that captures the causal dependencies in recommender systems under temporal distribution shift (TDS) settings.

- s<sub>u</sub> and s<sub>i</sub>: the abstract aggregated variables that contains the semantically stable information of user and item, respectively, e.g., the category of an item, which is relatively stable over time.
- v<sub>u</sub> and v<sub>i</sub>: the abstract aggregated time-varying variable for user
   u and item i, respectively, e.g., fluctuated item sales counts.
- z<sub>u</sub> and z<sub>i</sub>: the latent variable (a.k.a., representation) for user u
  and item i, respectively, determined by both s and v.
- x<sub>u</sub> and x<sub>i</sub>: the observed feature of user u and item i, respectively, determined by the latent variable z<sub>u</sub> and z<sub>i</sub>.
- y<sub>u,i</sub>: the interaction variable (e.g. click or conversion) between user u and item i, determined by both z<sub>u</sub> and z<sub>i</sub>.

From this process, we see three main paths driving TDS: 1)  $\mathbf{v}_u \to \mathbf{z}_u \to \mathbf{x}_u$  leads to the shift in user covariates  $\mathbf{x}_u$ ; 2)  $\mathbf{v}_i \to \mathbf{z}_i \to \mathbf{x}_i$  leads to the shift in item covariates  $\mathbf{x}_i$ ; 3)  $\mathbf{v}_u \to \mathbf{z}_u \to \mathbf{y}_{u,i} \leftarrow \mathbf{z}_i \leftarrow \mathbf{v}_i$  can lead to spurious correlations captured by a model. Collectively, these paths induce the joint distribution shift:  $p_{T-1}(\mathbf{x}_u, \mathbf{x}_i, \mathbf{y}_{u,i}) \neq p_T(\mathbf{x}_u, \mathbf{x}_i, \mathbf{y}_{u,i})$ , violating the i.i.d. assumption fundamental to Empirical Risk Minimization (ERM). For example, consider the scenario in Figure 1, on a regular day (T-1), users rarely purchase overpriced luxury items. Next, on a promotion day (T), heavy discounts and advertising  $(\mathbf{v})$  significantly increase their sales. ERM models trained

on  $p_{T-1}$  memorizes past patterns and fails to adapt, mispredicting user behaviors at promotion when pricing dynamics shift.

To improve generalization under temporal distribution shift (TDS), our objective is to retain the stable, informative factors while filtering out time-varying noise. This is enabled by an extended training distribution, constructed via augmentation to simulate realistic shifting patterns. Formally, grounded in the causal graph presented in Figure 1, we define the extended distribution as:  $p_{\mathcal{T}|\mathbf{s}_u,\mathbf{s}_i,\mathbf{v}_u,\mathbf{v}_i}$ , where  $\mathcal{T}$  denotes the augmented temporal support designed to reflect distributional changes (details provided in Section 3.3). Under this causal generative process, our learning objective becomes maximizing the conditional likelihood given the stable factors  $\mathbf{s}$ , using samples drawn from the enriched distribution.

$$\max_{\theta} \mathbb{E}_{(\mathbf{x}_u, \mathbf{x}_i, \mathbf{y}_{u,i}, \mathbf{s}_u, \mathbf{s}_i) \sim p_{\mathcal{T}|\mathbf{s}_u, \mathbf{s}_i, \mathbf{v}_u, \mathbf{v}_i}} [\log p_{\theta}(\mathbf{x}_u, \mathbf{x}_i, \mathbf{y}_{u,i}|\mathbf{s}_u, \mathbf{s}_i)], \quad (1)$$

where  $\mathbf{s}_u$  and  $\mathbf{s}_i$  denote the stable latent factors governing the generation of user and item covariates, respectively. These factors determine which samples share the same underlying semantics, and are implicitly realized through the augmentation strategy  $\mathcal{T}$ . Similar to self-supervised learning, we treat augmented views of the same base sample as sharing the same stable factors  $\mathbf{s}$ , whereas views of different base samples within a batch are assumed to correspond to different  $\mathbf{s}$ . This design encourages the model to preserve invariant semantic content while filtering out sample-specific temporal noise introduced through  $\mathbf{v}_u$  and  $\mathbf{v}_i$ .

To optimize Eqn. (1), we derive an Evidence Lower Bound [2] based on the causal generating process in Figure 1 (see derivation in Appendix A.1) as:

$$\max_{\theta} \mathbb{E}_{(\mathbf{x}_{u}, \mathbf{x}_{i}, \mathbf{y}_{u, i}, \mathbf{s}_{u}, \mathbf{s}_{i}) \sim p_{T|\mathbf{s}_{u}, \mathbf{s}_{i}, \mathbf{v}_{u}, \mathbf{v}_{i}}} [\log p_{\theta}(\mathbf{x}_{u}, \mathbf{x}_{i}, \mathbf{y}_{u, i}|\mathbf{s}_{u}, \mathbf{s}_{i})]$$

$$\geq \max_{\theta, \phi} \mathbb{E}_{(\mathbf{x}_{u}, \mathbf{x}_{i}, \mathbf{y}_{u, i}, \mathbf{s}_{u}, \mathbf{s}_{i}) \sim p_{T|\mathbf{s}_{u}, \mathbf{s}_{i}, \mathbf{v}_{u}, \mathbf{v}_{i}}} [\mathbb{E}_{\mathbf{z}_{u} \sim q_{\phi}(\mathbf{z}_{u}|\mathbf{x}_{u}), \mathbf{z}_{i} \sim q_{\phi}(\mathbf{z}_{i}|\mathbf{x}_{i})} [$$

$$\log p_{\theta}(\mathbf{x}_{u}|\mathbf{z}_{u}) + \log p_{\theta}(\mathbf{x}_{i}|\mathbf{z}_{i}) - \log q_{\phi}(\mathbf{z}_{u}|\mathbf{x}_{u}) - \log q_{\phi}(\mathbf{z}_{i}|\mathbf{x}_{i})$$

$$= \underbrace{\operatorname{entropy term}}_{\text{prodictive term}} + \underbrace{\log p_{\theta}(\mathbf{y}_{u, i}|\mathbf{z}_{u}, \mathbf{z}_{i})}_{\text{predictive term}} + \underbrace{\log p_{\theta}(\mathbf{z}_{u}|\mathbf{s}_{u}) + \log p_{\theta}(\mathbf{z}_{i}|\mathbf{s}_{i})}_{\text{prior term}} ]]$$

where  $q_{\phi}(\mathbf{z}_u|\mathbf{x}_u)$  and  $q_{\phi}(\mathbf{z}_i|\mathbf{x}_i)$  are the approximated posteriors of  $p(\mathbf{z}_u|\mathbf{x}_i)$  and  $p(\mathbf{z}_u|\mathbf{x}_i)$  parameterized by  $\phi$ . The ELBO can be

interpreted as four terms: *reconstruction, entropy, predictive, and prior terms*. For clarity, we group the reconstruction term, entropy term, and prior term into a **self-supervised component**, while the predictive term constitutes the **supervised component**.

*3.2.1 Self-Supervised Component.* We now provide explanations for each term and introduce tractable optimization objectives to construct the loss function for the self-supervised component.

**Prior term.** To ensure robustness against TDS, we enforce view-invariant representation learning. For a given user-item pair (u, i), various data views arise due to different strengths of time-varying factors  $\mathbf{v}_u$ ,  $\mathbf{v}_i$ . The prior term ensures that representations from all such views collapse toward the same prior distributions:  $p(\mathbf{z}_u|\mathbf{s})$ ,  $p(\mathbf{z}_i|\mathbf{s})$ . This process eliminates view-specific temporal noise, encouraging  $\mathbf{z}_u$  and  $\mathbf{z}_i$  capture only time-invariant user and item characteristics.

Formally, we assume  $q_{\phi}(\mathbf{z}_u|\mathbf{x}_u) = \mathcal{N}(f_{\phi_u}(\mathbf{x}_u), \mathbf{I})$  and  $q_{\phi}(\mathbf{z}_i|\mathbf{x}_i) = \mathcal{N}(f_{\phi_i}(\mathbf{x}_i), \mathbf{I})$ . Here,  $f_{\phi_u}$  and  $f_{\phi_i}$  are neural networks that estimate the mean representations, while the variance is fixed to I for training stability. For efficient sampling, we apply the reparameterization trick [27] with auxiliary noise  $\epsilon_u \sim \mathcal{N}(\mathbf{0}, \mathbf{I})$  and  $\epsilon_i \sim \mathcal{N}(\mathbf{0}, \mathbf{I})$ , yielding:  $\mathbf{z}_u = f_{\phi_u}(\mathbf{x}_u) + \mathbf{I}\epsilon_u$  and  $\mathbf{z}_i = f_{\phi_i}(\mathbf{x}_i) + \mathbf{I}\epsilon_i$ . Further, we assume the prior distributions  $p(\mathbf{z}_u|\mathbf{s}_u, \mathbf{v}_u)$  and  $p(\mathbf{z}_i|\mathbf{s}_i, \mathbf{v}_i)$  follow Gaussian distributions. Under this assumption, the prior loss is given by:

$$\mathcal{L}_{prior} = \mathcal{L}_{MSE}(\mathbf{z}_u, \overline{\mathbf{z}}_u) + \mathcal{L}_{MSE}(\mathbf{z}_i, \overline{\mathbf{z}}_i), \tag{3}$$

where  $\overline{\mathbf{z}}_u = \sum_{j=1}^J \mathbf{z}_u^j$  and  $\overline{\mathbf{z}}_i = \sum_{j=1}^J \mathbf{z}_i^j$ , averaged over J data views  $\{\mathbf{x}_u^j, \mathbf{x}_i^j\}_{j=1}^J$ . The derivation of Eqn. (3) is given in Appendix A.3. **Entropy term** controls the variance the the latent variable  $\mathbf{z}$ . Keeping a proper entropy can help avoid the collapse of  $\mathbf{z}$  to some extent [2]. Since  $\mathbf{z}_u$  and  $\mathbf{z}_i$  are Gaussian with unit variance (as mentioned in prior term), the entropy becomes a constant and contributes 0 to the gradient, thus can be canceled out.

**Reconstruction term** ensures that the latent representations  $\mathbf{z}_u$  and  $\mathbf{z}_i$  retain individual-specific information by reconstructing the original user and item features  $\mathbf{x}_u$  and  $\mathbf{x}_i$ . To achieve this, we employ deterministic neural networks  $f_{\theta_u}$  and  $f_{\theta_i}$  to to reconstruct the input covariates from the latent space:  $\hat{\mathbf{x}}_u = f_{\theta_u}(\mathbf{z}_u)$  and  $\hat{\mathbf{x}}_i = f_{\theta_i}(\mathbf{z}_i)$ . We optimize the reconstruction objective using the MSE loss:

$$\mathcal{L}_{recon} = \mathcal{L}_{MSE}(\hat{\mathbf{x}}_u, \mathbf{x}_u) + \mathcal{L}_{MSE}(\hat{\mathbf{x}}_i, \mathbf{x}_i). \tag{4}$$

Combining them yields the self-supervised objective:

$$\min_{\phi,\theta} \mathbb{E}_{(\mathbf{x}_u, \mathbf{x}_i, \mathbf{s}_u, \mathbf{s}_i) \sim p_{\mathcal{T}|\mathbf{s}_u, \mathbf{s}_i, \mathbf{v}_u, \mathbf{v}_i}} [\mathcal{L}_{recon} + \mathcal{L}_{prior}]. \tag{5}$$

3.2.2 Supervised Component. The **predictive term** aligns latent representations  $\mathbf{z}_u$  and  $\mathbf{z}_i$  with the target interaction  $y_{u,i}$ , which can be interpreted as any recommendation tasks (e.g., click prediction) modeled by corresponding deterministic network  $f_{\theta_{u,i}}$ . To ensure the training-inference consistency and ranking capability, we use the deterministic means  $f_{\phi_u}(\mathbf{x}_u)$  and  $f_{\phi_i}(\mathbf{x}_i)$  (extracted from truly observed data  $\mathbf{x}_u, \mathbf{x}_i$ ). The supervised objective then is given by :

$$\min_{\phi,\theta} \mathbb{E}_{(\mathbf{x}_u,\mathbf{x}_i,\mathbf{y}_{u,i}) \sim p_{train}} [\mathcal{L}_{pred}], \tag{6}$$

where  $\mathcal{L}_{pred} = \mathcal{L}_{pred}(f_{\theta_{u,i}}(f_{\phi_u}(\mathbf{x}_u), f_{\phi_i}(\mathbf{x}_i)), \mathbf{y}_{u,i})$  is the task-specific loss, and  $p_{train}$  is the truly observed distribution (subset of  $\mathcal{T}$ ).

Combining the self-supervised and supervised components yields the total loss of our framework:

$$\min_{\phi,\theta} \mathbb{E}_{(\mathbf{x}_{u},\mathbf{x}_{i},\mathbf{y}_{u,i}) \sim p_{train}} [\mathcal{L}_{pred}] 
+ \alpha \mathbb{E}_{(\mathbf{x}_{u},\mathbf{x}_{i},s_{u},s_{i}) \sim p_{T|s_{u},s_{i},\mathbf{y}_{u},\mathbf{y}_{i}}} [\mathcal{L}_{recon} + \mathcal{L}_{prior}],$$
(7)

where  $\phi = (\phi_u, \phi_i)$ ,  $\theta = (\theta_u, \theta_i, \theta_{u,i})$ , and  $\alpha$  is a hyperparameter that balances the self-supervised and supervised components.

# 3.3 Data Augmentation and Training Pipeline

As discussed in Section 3.2, our optimization framework would ideally handle TDS if we could observe multiple parallel counterfactual worlds, each reflecting different realizations of time-varying factors. Since this is infeasible, we design a data augmentation strategy that generates J augmented views  $(\mathbf{x}_u^j, \mathbf{x}_i^j)_{j=1}^J = \mathcal{T}(\mathbf{x}_u, \mathbf{x}_i | \mathbf{s}_u, \mathbf{s}_i, \mathbf{v}_u, \mathbf{v}_i)$ , with two goals: (1) approximate realistic temporal fluctuations and (2) preserve a relatively stable core.

Guided by the empirical findings in Section 3.1, we craft feature-type–specific augmentations and add a lightweight random-fusion scheme to produce multiple views on the fly. Finally, we integrate this augmentation into a streamlined training pipeline that pairs naturally with our proposed loss, yielding both efficiency and robustness against TDS.

3.3.1 Statistical Features. fluctuate around a mean. To mimic this, we perturb them within a controlled range while keeping their global distribution intact. Because different statistics have different scales, we first bucketize each feature into equal-width bins. Given an original bucket index  $B_i$ , we sample a perturbed index:

$$B'_{i} = \min(\max(B_{i} + \epsilon, 0), B_{max})$$
 s.t.  $\epsilon \sim \mathcal{U}\{-r, r\},$ 

where  $B_{\text{max}}$  is the max bin index and r controls perturbation strength.

- 3.3.2 Sequential Features. Historical action sequences also fluctuate in length and content. To reflect this, we adopt random masking (akin to masked language modeling [11, 35]) so the model learns contextual signals rather than memorizing specific subsequences. Concretely, we sample a binary mask  $\mathbf{m} \sim \text{Bern}(p_{seq})$ , where  $p_{seq}$  is the masking probability.
- 3.3.3 Categorical Features. Categorical distributions drift continuously over time, risking overfitting to transient modes. We therefore apply embedding dropout with rate  $p_{cate}$ , randomly zeroing embeddings to prevent reliance on any single categorical snapshot.
- 3.3.4 Global Perturbation Selection. To avoid overly aggressive augmentation that would push samples outside realistic temporal support, we perturb only a random subset of features per sample. This "global perturbation cap," inspired by vision augmentations such as Random Erasing and Cutout [12, 54], keeps augmented data faithful to real-world TDS patterns.
- 3.3.5 Training Pipeline. Because our augmentations are lightweight, we generate J augmented views on the fly for each batch. We then compute all loss components and optimize them jointly. Crucially, this obviates the need to cache and mix long spans of historical data  $\mathcal{D}t \leq T$ , avoiding storage-heavy multi-span training. The resulting framework, ELBO<sub>TDS</sub>, plugs seamlessly into existing incremental recommendation pipelines with minimal code changes (see Figure 2(d) and AppendixB.2 for implementation details).

## 3.4 Collapse Analysis of InfoNCE

In this section, we theoretically compare ELBO $_{TDS}$  with InfoNCE, offering intuition for why ELBO $_{TDS}$  can perform better under TDS. We present a lower bound for InfoNCE, stated in Proposition 1.

PROPOSITION 1. Let  $\mathbf{x}_u$  and  $\mathbf{x}_i$  be user and item features with their respective augmented views  $\mathbf{X}_u = \{\mathbf{x}_u, \mathbf{x}_u^{+,0}, \mathbf{x}_u^{-,1}, ..., \mathbf{x}_u^{-,k}\}$  and  $\mathbf{X}_i = \{\mathbf{x}_i, \mathbf{x}_i^{+,0}, \mathbf{x}_i^{-,1}, ..., \mathbf{x}_i^{-,k}\}$ . the InfoNCE loss upper bounds the following expression:

$$\mathcal{L}_{InfoNCE}^{u} + \mathcal{L}_{InfoNCE}^{i}$$

$$\geq -\mathbb{E}_{\mathbf{x}_{u},\mathbf{x}_{i}}[\mathbb{E}_{\mathbf{z}_{u},\mathbf{z}_{i}}[\log p(\mathbf{z}_{u}|\mathbf{s}_{u}) + \log p(\mathbf{z}_{u}|\mathbf{s}_{i}) - \log p(\mathbf{z}_{u}) - \log p(\mathbf{z}_{i})]] - c$$
(8)

where  $c = 2 \log k$  and k is the number of negative samples.

The proof is given in Appendix A.2. Proposition 1 shows that InfoNCE actually minimizes an upper bound of an ELBO-like objective, where the reconstruction term is replaced by entropy penalties  $-\log p(\mathbf{z}_u)$  and  $-\log p(\mathbf{z}_i)$ . Although these entropy terms promote uniformity and discourage severe over-clustering, they do not explicitly enforce the retention of per-sample, idiosyncratic details, leaving room for harmful representation collapse.

In e-commerce recommendation, such fine-grained details often prove crucial for downstream tasks, such as personalized ranking. As an illustrative example, suppose multiple users share a preference for iPhones (a common semantic theme), yet some users are notably price-insensitive, preferring new models over older versions. If the representation learner only clusters iPhone fans as a group without constraints on personalized information preservation, it may overlook these individual nuances—leading to less accurate recommendations. By contrast, a reconstruction-based approach retains these subtle distinctions, enabling more precise personalization.

**Remark.** In contrast to InfoNCE, the reconstruction terms  $p_{\theta}(\mathbf{x}_u|\mathbf{z}_u)$  and  $p_{\theta}(\mathbf{x}_i|\mathbf{z}_i)$  of ELBO<sub>TDS</sub> promote individual-level feature preservation. This preservation is key to precise item recommendations.

# 4 Experiment

In this section, we conduct extensive experiments in both offline and online settings.

# 4.1 Experiment Settings

4.1.1 Datasets. We evaluate our model on datasets collected from real online traffic in Shopee's Primary Search scenario (referred to as **Shopee-Main**), where recommendation techniques power personalized search experiences. It aggregates multi-region data from Southeast Asia over 40 days, including about 200 well-engineered features spanning statistical, sequential, and categorical types. It includes three types of user feedback—click, add-to-cart, and purchase—and is structured into user sessions to support listwise modeling. The dataset contains approximately 30 billion samples, making it a industry-scale benchmark for studying TDS problem.

To facilitate reproducibility, we release a subset of Shopee-Main, named **Shopee-Small**, which consists of 13 consecutive days of data from a smaller region without any sampling. In addition, we

Table 1: Multi-Task listwise ranking on Shopee-Small on MLP backbone and Cross-entropy&ListNet loss.

backbone: MLP	Click		Add T	o Cart	Purchase	
loss: CE&ListNet [5]	AUC	GAUC	AUC	GAUC	AUC	GAUC
ERM	0.7977	0.7910	0.8494	0.7966	0.8920	0.8228
Aug	0.7982	0.7905	0.8497	0.7979	0.8917	0.8249
IRM	0.7775	0.7715	0.8094	0.7624	0.8421	0.7831
V-REx	0.7827	0.7764	0.8155	0.7708	0.8446	0.7898
RVP	0.7821	0.7756	0.8134	0.7676	0.8419	0.7838
DINO4Rec	0.7996	0.7914	0.8475	0.7961	0.8904	0.8218
SSL4Rec	0.8005	0.7932	0.8496	0.7973	0.8906	0.8213
SSL4Rec*	0.8012	0.7941	0.8490	0.7985	0.8894	0.8228
$ELBO_{TDS}$	0.8042	0.7976	0.8528	0.8037	0.8934	0.8297
ELBO <sub>TDS</sub> +stat	0.8040	0.7974	0.8511	0.8021	0.8935	0.8294
$ELBO_{TDS}+seq$	0.8036	0.7967	0.8520	0.8029	0.8930	0.8295
ELBO <sub>TDS</sub> +cate	0.8020	0.7957	0.8510	0.8019	0.8935	0.8285

identify **KuaiRand-1K**, the only suitable dataset publicly available for TDS, which contains nearly 100 well-engineered features with disclosed semantic meanings, allowing targeted augmentation. KuaiRand-1K also provides timestamps for user-item interactions, enabling chronological data partitioning for TDS evaluation.

For Shopee-Main and Shopee-Small, we use the last day for testing, the second-last day for validation, and the remaining days for training. For KuaiRand-1K, we divide the dataset into 10 equal-sized time spans, using the last span for testing, the second-last for validation, and the rest for training. We evaluate KuaiRand-1K on two feedback types: is\_like and is\_follow, conducting both single-task and multi-task evaluations (Details in Appendix B.1).

4.1.2 Baselines. Since we piorneer in explicitly addressing TDS, we compare ELBO<sub>TDS</sub> against SOTA approaches adapted to TDS: ERM is an implementation of incremental empirical risk minimization prevalent in industrial practice. Direct Augmentation (Aug) trains directly on the augmented distribution without our probabilistic objective. IRM[1], V-REx[29], and RVP [32] are SOTA invariant learning methods. SSL4Rec [59] is a self-supervised learning (SSL) method that only augments item-specific features, aiming to enhance long-tail item generalization. SSL4Rec\* [53] is an enhanced version of SSL4Rec that augments all feature types, same as ELBO<sub>TDS</sub>, serving as a stronger baseline. Inspired by SSL4Rec and the success of Dinov2 [40], we use Dinov2 as an auxiliary task for supervised tasks, namely Dino4Rec.

4.1.3 Evaluation Metrics. We use AUC to measure point-wise ranking effectiveness [38, 44] and GAUC to evaluates list-wise ranking performance [5]. We adopt GMV/User (Gross Merchandise Value per User) to assess business impact in online A/B tests.

4.1.4 Implementations. We implement all methods using a twintower architecture [50], ensuring a fair comparison by keeping the backbone architecture identical across all baselines. Additionally, we perform a grid search to tune hyperparameters for all methods. Further implementation details are provided in Appendix B.2.

### 4.2 Offline Results and Analyses

4.2.1 RQ1&2: Overall Performance & Downstream Task Evaluation. We evaluate ELBO<sub>TDS</sub> across three experimental settings: Single- and Multi-task pointwise ranking (KuaiRand-1K), and

backbone: MLP	KuaiRand-1	K single-task	KuaiRand-1K multi-task					
	is_like		is_	like	is_fo	is_follow		
Loss: Cross Entropy (CE)	AUC	GAUC	AUC	GAUC	AUC	GAUC		
ERM	0.9053±0.0029	0.5086±0.0053	0.9015±0.0029	0.5025±0.0042	0.7816±0.0134	0.5016±0.0014		
Aug	0.9032±0.0035	$0.5013 \pm 0.0044$	$0.8947 \pm 0.0032$	$0.5009 \pm 0.0046$	0.7952±0.0045	0.4997±0.0039		
IRM	0.9043±0.0019	$0.5079 \pm 0.0027$	0.9034±0.0008	$0.5008 \pm 0.0044$	0.7816±0.0161	$0.5016 \pm 0.0021$		
V-REx	0.9046±0.0013	$0.5060 \pm 0.0034$	0.9034±0.0004	$0.5022 \pm 0.0034$	$0.7779 \pm 0.0204$	$0.5008 \pm 0.0003$		
RVP	$0.9049 \pm 0.0022$	0.5093±0.0047	0.9035±0.0040	$0.5020 \pm 0.0033$	0.7783±0.0113	0.5011±0.0015		
Dino4Rec	0.9046±0.0017	$0.5066 \pm 0.0034$	0.9017±0.0017	$0.5020 \pm 0.0041$	$0.7841 \pm 0.0032$	0.5011±0.0013		
SSL4Rec	0.9001±0.0007	$0.5042 \pm 0.0066$	$0.9014 \pm 0.0024$	$0.5015 \pm 0.0062$	0.7837±0.0061	$0.5020 \pm 0.0024$		
SSL4Rec*	0.9072±0.0006	$0.5020 \pm 0.0054$	$0.9060 \pm 0.0025$	$0.4986 \pm 0.0042$	$0.8101 \pm 0.0050$	0.4998±0.0047		
$ELBO_{TDS}$	0.9112±0.0008	0.5191±0.0037	0.9093±0.0011	0.5101±0.0065	$0.8260 \pm 0.0030$	$0.5024 \pm 0.0013$		

Table 2: Single- and multi-task ranking performance on the Kuairand-1K dataset on MLP backbone and cross entropy loss.

Multi-task listwise ranking (Shopee-Small). The results (Table 1 and Table 2), reveal several key insights:

- (i) ELBO<sub>TDS</sub> consistently outperforms all baselines across datasets and tasks under TDS. These results validate two key insights: 1. **TDS is a universal challenge** across different types of recommender systems, e.g., video recommendations (KuaiRand-1K) and e-commerce (Shopee-Small). 2. **ELBO<sub>TDS</sub> is highly adaptable**, showing strong generalization over diverse modalities and tasks.
- (ii) Invariant learning struggles with TDS, especially in large-scale. IRM, V-REx, and RVP perform on par with ERM on KuaiRand-1K, but significantly worse than ERM on Shopee-Small. This suggests that existing invariant learning methods are ineffective for TDS, due to two fundamental reasons: (a) They fail to capture the true time-invariant factors. (b) They overfit on historical patterns due to multiple passes over past time spans. This aligns with findings from prior work [26, 64], showing that training more than 1 epoch directly causes overfitting. In contrast, ELBO<sub>TDS</sub> and SSL methods avoid overfitting since they process each day's data only once.
- (iii) SSL improves dense feedback tasks but struggles with sparse targets. Dino4Rec, SSL4Rec, and SSL4Rec\* perform better than ERM on dense feedback (e.g., is\_like, click) but show no improvement or even degrade performance on sparse targets (e.g., purchase).

We attribute this to the representation collapse issue (Section 3.4). Prior SSL methods encourage clustering of similar samples, improving generalization for frequent interactions (e.g., clicks). However, predicting rare behaviors (e.g., purchases, follows) demands capturing subtle but critical factors from extremely sparse positive samples. These SSL loss does not explicitly enforce this, leading to oversuppression of rare sample characteristics. In contrast, ELBO<sub>TDS</sub> preserves individual nuances through its reconstruction term.

- (iv)  $ELBO_{TDS}$  maintains strong GAUC performance even without listwise losses. This further confirms the representation collapse issue in prior SSL methods, where user-specific preference details are lost. Without explicit constraints, they suppresses intra-cluster variance, reducing personalization. Listwise losses partially recover this, but  $ELBO_{TDS}$  inherently preserves these details through its reconstruction term, leading to superior ranking performance.
- (v) ELBO<sub>TDS</sub> maintains a stable uplift over ERM throughout training. ERM, Dino4Rec, SSL4Rec, SSL4Rec\*, and ELBO<sub>TDS</sub> all show positive scaling trends, where next-day test AUC and GAUC improve over time in daily incremental training on Shopee-Small (Figure 3). However, we observe three key trends: (a) Invariant

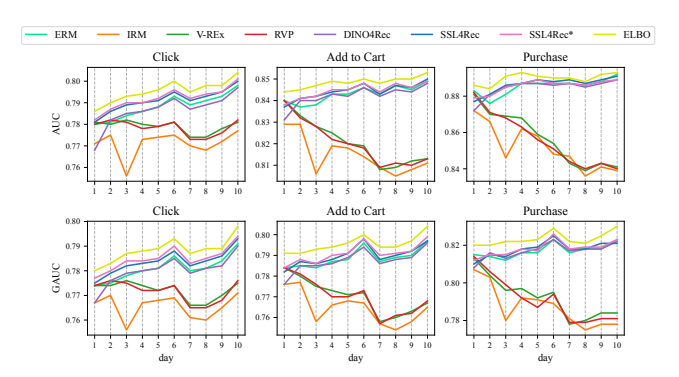


Figure 3: Scaling-over-time capability on Shopee-Small. Each day's checkpoints are tested on untrained next day's data.

learning methods deteriorate over time, reinforcing their overfitting to outdated patterns. (b) SSL methods initially improve over ERM but gradually lose their advantage, especially on sparse targets. This demonstrates that incremental training may aggravate their representation collapse and loss in personalized information. (c) The higher AUC than Aug demonstrates the effectiveness of ELBO $_{\mathrm{TDS}}$  rather than just benefiting from data augmentation.

In contrast, ELBO $_{\rm TDS}$  consistently maintains its uplift over ERM, demonstrating long-term stability and adaptability to evolving data distributions. This robustness is crucial for practical deployment in dynamic real-world recommender systems.

4.2.2 RQ3: Ablation Study. We conduct an ablation study to evaluate the individual contributions of different augmentation strategies on Shopee-Small (Table 1). Key insights are as follows: (i). Each augmentation strategy improves over ERM when combined with ELBO<sub>TDS</sub>. Further, SSL4Rec is also enhanced with our full augmentation (SSL4Rec\*). These validate that our design effectively simulates real-world data fluctuations caused by TDS. (ii) Statistical feature augmentation has the highest impact, while categorical feature augmentation contributes the least. This suggests that statistical features (e.g., CTRs) fluctuate more significantly over time and thus require stronger regularization. (iii) The combined effect of all augmentations is not strictly additive, meaning the overall performance gain is smaller than the sum of individual contributions. This may be due to the inefficiency in the fusion of augmentations from different feature types, leading to diminishing returns. More

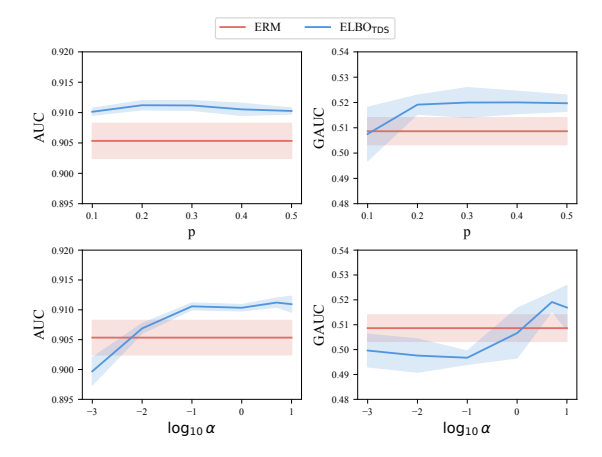


Figure 4: Parameter sensitivity of p and  $\alpha$  on Kuairand-1K.

Table 3: Mean daily uplift over ERM on Shopee-Main.

backbone: MLP	Click		Add T	o Cart	Purchase	
loss: CE&ListNet[5]	AUC	GAUC	AUC	GAUC	AUC	GAUC
DINO4Rec	+0.05%	+0.01%	-0.02%	-0.01%	-0.02%	+0.05%
SSL4Rec*	+0.51%	+0.34%	+0.42%	+0.31%	+0.34%	+0.28%
ELBO <sub>TDS</sub>	+0.93%	+1.02%	+0.63%	+0.71%	+0.69%	+0.73%

sophisticated aggregation mechanism should be investigated. We leave a deeper investigation into this effect for future work.

4.2.3 **RQ4: Hyperparameter Sensitivity**. We analyze the impact of two key hyperparameters: perturbation strength (p) and self-supervised loss weight ( $\alpha$ ) across both datasets. The results, shown in Figure 4 and 5, reveal the following insights: (i) Denser targets (e.g., click) are less sensitive to perturbation strength (p), whereas sparser targets (e.g., purchase) are more sensitive. Sparse targets depend on rare positive samples, making them more reliant on effective data augmentation. Insufficient perturbation fails to adequately simulate TDS, while excessive perturbation injects noises, degrading supervision quality. This highlights the importance of tuning p to balance robustness and noise control. (ii) KuaiRand-1K benefits from a higher  $\alpha$ , while Shopee performs better with a lower α. KuaiRand-1K is a small, aggressively sampled dataset, which leads to insufficient fitting for supervised tasks. This also explains why invariant learning does not overfit on KuaiRand-1K. In this case, stronger self-supervision compensates for insufficient labeled data, improving robustness to TDS. Conversely, Shopee-Small contains ample training data, reducing the reliance for self-supervision. A lower  $\alpha$  allows the model to focus more on supervised learning, ensuring better adaptation to the latest interactions.

#### 4.3 Online A/B Test Results (RQ5)

4.3.1 **Pretraining on Shopee-Main**. Due to resource constraints and the fact that models have not fully converged on Shopee-Small, we select Dino4Rec, SSL4Rec\*, and ELBO<sub>TDS</sub> for extended training on Shopee-Main until convergence, comparing them against incremental ERM. We record next-day test AUC/GAUC uplift over ERM and report the average in Table 3. The findings show that ELBO<sub>TDS</sub> consistently maintains a significant improvement over long-term incremental training, outperforming both SSL baselines.

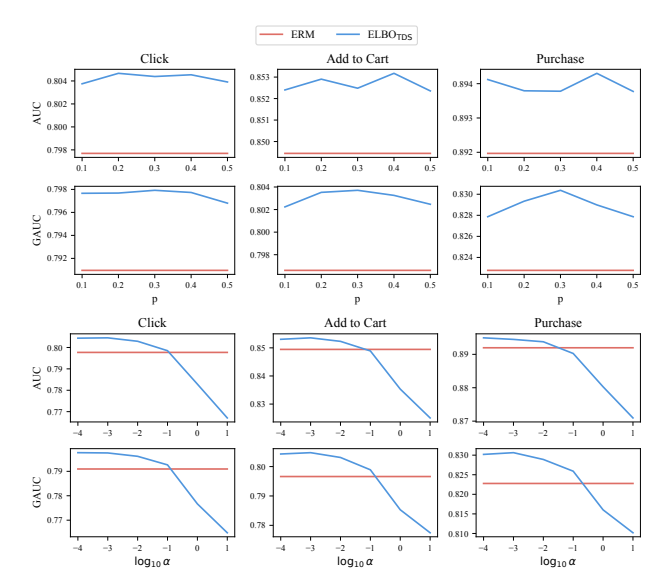


Figure 5: Parameter sensitivity of p and  $\alpha$  on Shopee-Small.

4.3.2 Online A/B Test Regarding Business Metric. To ensure a rigorous online evaluation, we conduct an A/B test with the following setup: (i) Shopee employs a cascading recommendation system [3] with multiple ranking stages, progressively filtering candidates from billions to hundreds. We integrate ELBO<sub>TDS</sub> into two key ranking stages: Coarse-Ranking and Ranking, allowing us to assess its impact on overall ranking quality. (ii) We allocate 10% of traffic to the baseline group (cascade ERM) and another 10% to the treatment group (cascade ELBO<sub>TDS</sub>) (iii) Our core evaluation metric is GMV per User (GMV/User), which directly correlates with platform revenue. However, our model is not explicitly optimized for GMV, we use the following GMV-oriented formula for ranking:

$$S = S' + \lambda S' \cdot Price, \quad S' = S_{click}^{\gamma_1} \cdot S_{purchase}^{\gamma_2},$$

where  $S_{click}$  and  $S_{purchase}$  are model predictions, and  $\lambda$ ,  $\gamma_1$ ,  $\gamma_2$  are hyperparameters tuned for optimal business performance. For efficiency, we omit add-to-cart prediction, streamlining the hyperparameter tuning process.

Over a two-week A/B test, ELBO<sub>TDS</sub> consistently outperforms the baseline, achieving: (1) +2.33% uplift in GMV/User, a significant gain for a single deployment. (2) +0.2% improvement in online human evaluations, which assess user experience and item relevance. Given these strong results, ELBO<sub>TDS</sub> has been fully deployed in Shopee Search, highlighting its scalability and robustness. See more details in Appendix B.2 and B.6.

4.3.3 Robustness Against Drastic Shift. During the two-week A/B test, a major single-day sales promotion took place on Shopee, significantly impacting user behavior. The event introduced extreme temporal shifts: Before the sales day, users engage more, clicking and adding items to their carts, but delay purchases to wait for discounts. On the sales day, a surge in purchases occurs as users execute planned transactions. After the sales day, overall interaction levels drop, reducing clicks, add-to-cart actions, and purchases.

To help incremental ERM adapt to such drastic shifts, platforms typically switch from daily training to hourly training to capture real-time fluctuations and reduce prediction loss. To assess

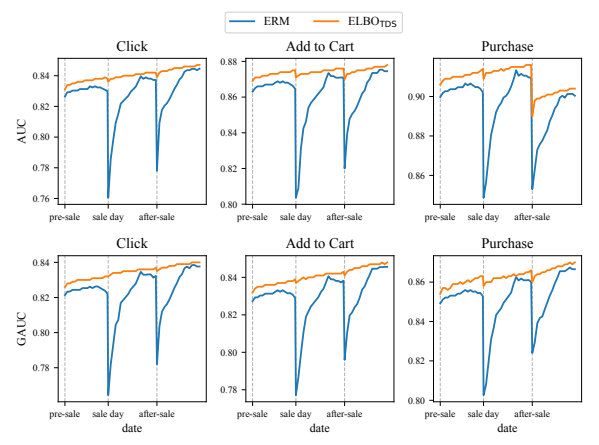


Figure 6: Hourly AUC/GAUC during Shopee's Promotion.

ELBO<sub>TDS</sub>'s robustness in such scenarios, we track next-hour test AUC/GAUC across the three-day period (before, during, and after the sale). The results, shown in Figure 6, reveal the following. (i) Incremental ERM experienced a sharp drop in AUC/GAUC, failing to adjust quickly to sudden shifts in user behavior. (ii) ELBO<sub>TDS</sub> maintained significantly better stability, with only a minor drop in performance at midnight. (iii) ERM eventually caught up later in the day, yet caused significant revenue loss already.

These results confirm ELBO<sub>TDS</sub>'s ability to generalize effectively across sudden market fluctuations, offering a robust solution without requiring frequent retraining or reactive fine-tuning.

#### 5 Related Work

Our work is closely related to recommender systems, out-of-distribution (OOD) generalization, and self-supervised learning (SSL).

Industrial Recommender Systems. Modern industrial recommender systems typically consist of sparse and dense components [61]. The sparse component utilizes embedding lookup tables to transform categorical features into dense representations, while the dense component models feature interactions to generate predictions. These systems leverage deep learning techniques and feature engineering strategies—including categorical, statistical, and sequential features—to enhance predictive accuracy [10, 17, 19, 37, 52]. Despite their success, they remain vulnerable to TDS.

OOD generalization. OOD generalization, a fundamental challenge in machine learning [33], aims to improve model robustness against distribution shifts. One class of methods, *unsupervised domain adaptation* [14, 34], aligns feature distributions between the source and target domains using unlabeled target data. However, in industrial recommender systems, future distributions are inaccessible. Another class of methods, *invariant learning*, seeks representations stable across different environments, enabling generalization to unseen data [1, 29, 32, 46]. Despite its theoretical appeal, invariant learning is impractical for real-world recommender systems due to: (i) Difficulty in Defining Environments. Unlike conventional domain generalization, where environments are predefined, temporal shifts in recommender systems occur at varying rates, making it unclear how to segment historical data into meaningful

environments. (ii) Historical Data Trade-off. Invariant learning requires sufficient environments to disentangle varying factors, but excessive historical data inflates computational costs and introduces outdated correlations.

**Self-supervised learning.** SSL, paired with data augmentation [28, 45, 48, 62], has emerged as a powerful paradigm for representation learning, broadly categorized into contrastive, non-contrastive, and generative methods. Contrastive Learning enforces similarity between augmented views of the same sample while pushing apart representations from different samples [7, 9, 24, 60], often using the InfoNCE loss [53]. Non-Contrastive Learning, including BYOL [18], SimSiam [8], and DINO [6, 40], avoids representation collapse using architectural techniques and distillation. Generative Learning mitigates collapse by introducing auxiliary tasks such as reconstructing perturbed views [2, 23, 58] or predicting data transformations [15]. In recommender systems, SSL has gained significant traction [43]. Notably, BUIR [30] employs a teacher-student framework akin to BYOL, while SelfCF [67] adopts a SimSiam-like structure for contrastive learning. SSL4Rec [59], the most relevant to our work, applies InfoNCE regularization to item embeddings to generalize to long-tail items and enhance prediction accuracy.

#### 6 Conclusion

In this work, we tackle the often-overlooked problem of temporal distribution shift (TDS) in recommender systems. We introduce  $\rm ELBO_{TDS}$ , a probabilistic framework that improves robustness in dynamic, real-world settings. The framework has two core components: (i) a simple yet effective data augmentation scheme that mimics temporal fluctuations to extend the training support; and (ii) a probabilistic objective—ELBO\_{TDS}—that exploits this extended distribution while avoiding representation collapse. The method is lightweight and plug-and-play, requiring minimal changes to existing recommender architectures and incremental training pipelines. Extensive offline experiments and online A/B tests demonstrate its superiority in practice. To spur further research, we will release the industrial-scale dataset used in our study.

#### References

- Martin Arjovsky, Léon Bottou, Ishaan Gulrajani, and David Lopez-Paz. 2020. Invariant Risk Minimization. arXiv:1907.02893 [stat.ML]
- [2] Alice Bizeul, Bernhard Schölkopf, and Carl Allen. 2024. A Probabilistic Model behind Self- Supervised Learning. <u>Transactions on Machine Learning Research</u> (2024). https://openreview.net/forum?id=QEwz7447tR
- [3] Robin Burke. 2002. Hybrid recommender systems: Survey and experiments. <u>User modeling and user-adapted interaction</u> 12 (2002), 331–370.
- [4] Zhe Cao, Tao Qin, Tie-Yan Liu, Ming-Feng Tsai, and Hang Li. 2007. Learning to rank: from pairwise approach to listwise approach. In Proceedings of the 24th International Conference on Machine Learning (Corvalis, Oregon, USA) (ICML '07). Association for Computing Machinery, New York, NY, USA, 129–136. https://doi.org/10.1145/1273496.1273513
- [5] Zhe Cao, Tao Qin, Tie-Yan Liu, Ming-Feng Tsai, and Hang Li. 2007. Learning to rank: from pairwise approach to listwise approach. In Proceedings of the 24th International Conference on Machine Learning (Corvalis, Oregon, USA) (ICML '07). Association for Computing Machinery, New York, NY, USA, 129–136. https://doi.org/10.1145/1273496.1273513
- [6] Mathilde Caron, Hugo Touvron, Ishan Misra, Hervé Jegou, Julien Mairal, Piotr Bojanowski, and Armand Joulin. 2021. Emerging Properties in Self-Supervised Vision Transformers. In 2021 IEEE/CVF International Conference on Computer Vision (ICCV). 9630–9640. https://doi.org/10.1109/ICCV48922.2021.00951
- [7] Xinlei Chen, Haoqi Fan, Ross Girshick, and Kaiming He. 2020. Improved Baselines with Momentum Contrastive Learning. arXiv:2003.04297 [cs.CV]
- [8] Xinlei Chen and Kaiming He. 2021. Exploring Simple Siamese Representation Learning. In 2021 IEEE/CVF Conference on Computer Vision and Pattern

- Recognition (CVPR). 15745–15753. https://doi.org/10.1109/CVPR46437.2021.
- [9] Xinlei Chen, Saining Xie, and Kaiming He. 2021. An Empirical Study of Training Self-Supervised Vision Transformers. In 2021 IEEE/CVF International Conference on Computer Vision (ICCV). 9620–9629. https://doi.org/10.1109/ ICCV48922.2021.00950
- [10] Heng-Tze Cheng, Levent Koc, Jeremiah Harmsen, Tal Shaked, Tushar Chandra, Hrishi Aradhye, Glen Anderson, Greg Corrado, Wei Chai, Mustafa Ispir, et al. 2016. Wide & deep learning for recommender systems. In <u>Proceedings of the 1st</u> workshop on deep learning for recommender systems. 7–10.
- [11] Jacob Devlin, Ming-Wei Chang, Kenton Lee, and Kristina Toutanova. 2019. BERT: Pre-training of Deep Bidirectional Transformers for Language Understanding. In Proceedings of the 2019 Conference of the North American Chapter of the Association for Computational Linguistics: Human Language Technologies, Volume 1 (Long and Short Papers). Association for Computational Linguistics, Minneapolis, Minnesota.
- [12] Alexey Dosovitskiy and Thomas Brox. 2016. Generating Images with Perceptual Similarity Metrics based on Deep Networks. In <u>Advances in Neural Information</u> Processing Systems, Vol. 29. Curran Associates, Inc.
- [13] Cong Fu, Kun Wang, Jiahua Wu, Yizhou Chen, Guangda Huzhang, Yabo Ni, Anxiang Zeng, and Zhiming Zhou. 2024. Residual Multi-Task Learner for Applied Ranking. In Proceedings of the 30th ACM SIGKDD Conference on Knowledge Discovery and Data Mining (Barcelona, Spain) (KDD '24). Association for Computing Machinery, New York, NY, USA, 4974–4985. https://doi.org/10.1145/3637528.3671523
- [14] Yaroslav Ganin, Evgeniya Ustinova, Hana Ajakan, Pascal Germain, Hugo Larochelle, François Laviolette, Mario March, and Victor Lempitsky. 2016. Domain-Adversarial Training of Neural Networks. <u>Journal of Machine Learning</u> Research 17, 59 (2016), 1–35.
- [15] Spyros Gidaris, Praveer Singh, and Nikos Komodakis. 2018. Unsupervised Representation Learning by Predicting Image Rotations. arXiv:1803.07728 [cs.CV]
- [16] Mark Granroth-Wilding and Stephen Clark. 2016. What Happens Next? Event Prediction Using a Compositional Neural Network Model. <u>Proceedings of the AAAI Conference on Artificial Intelligence</u> 30, 1 (Mar. 2016). https://doi.org/10.1609/aaai.v30i1.10344
- [17] Mihajlo Grbovic and Haibin Cheng. 2018. Real-time personalization using embeddings for search ranking at airbnb. In Proceedings of the 24th ACM SIGKDD international conference on knowledge discovery & data mining 311–320
- international conference on knowledge discovery & data mining. 311–320.

  [18] Jean-Bastien Grill, Florian Strub, Florent Altché, Corentin Tallec, Pierre Richemond, Elena Buchatskaya, Carl Doersch, Bernardo Avila Pires, Zhaohan Guo, Mohammad Gheshlaghi Azar, Bilal Piot, koray kavukcuoglu, Remi Munos, and Michal Valko. 2020. Bootstrap Your Own Latent A New Approach to Self-Supervised Learning. In Advances in Neural Information Processing Systems, H. Larochelle, M. Ranzato, R. Hadsell, M.F. Balcan, and H. Lin (Eds.), Vol. 33. Curran Associates, Inc., 21271–21284.
- [19] Huifeng Guo, Ruiming Tang, Yunming Ye, Zhenguo Li, and Xiuqiang He. 2017. DeepFM: a factorization-machine based neural network for CTR prediction. arXiv preprint arXiv:1703.04247 (2017).
- [20] Jiawei Han, Jian Pei, and Yiwen Yin. 2000. Mining frequent patterns without candidate generation. ACM sigmod record 29, 2 (2000), 1–12.
- [21] F. Maxwell Harper and Joseph A. Konstan. 2015. The MovieLens Datasets: History and Context. <u>ACM Transactions on Interactive Intelligent Systems (TiiS)</u> 5, 4 (2015).
- [22] GM Harshvardhan, Mahendra Kumar Gourisaria, Manjusha Pandey, and Siddharth Swarup Rautaray. 2020. A comprehensive survey and analysis of generative models in machine learning. <u>Computer Science Review</u> 38 (2020), 100285.
- [23] Kaiming He, Xinlei Chen, Saining Xie, Yanghao Li, Piotr Dollár, and Ross Girshick. 2022. Masked Autoencoders Are Scalable Vision Learners. In 2022 IEEE/CVF Conference on Computer Vision and Pattern Recognition (CVPR). 15979–15988. https://doi.org/10.1109/CVPR52688.2022.01553
- [24] Kaiming He, Haoqi Fan, Yuxin Wu, Saining Xie, and Ross Girshick. 2020. Momentum Contrast for Unsupervised Visual Representation Learning. In 2020 IEEE/CVF Conference on Computer Vision and Pattern Recognition (CVPR). 9726–9735. https://doi.org/10.1109/CVPR42600.2020.00975
- [25] Balázs Hidasi and Alexandros Karatzoglou. 2018. Recurrent Neural Networks with Top-k Gains for Session-based Recommendations. In <u>Proceedings</u> of the 27th ACM International Conference on Information and <u>Knowledge Management</u> (Torino, Italy) (<u>CIKM '18</u>). Association for Computing Machinery, New York, NY, USA, 843–852. https://doi.org/10.1145/3269206.3271761
- [26] Yi-Ping Hsu, Po-Wei Wang, Chantat Eksombatchai, and Jiajing Xu. 2024. Taming the One-Epoch Phenomenon in Online Recommendation System by Two-stage Contrastive ID Pre-training. In <u>Proceedings of the 18th ACM Conference on</u> Recommender Systems. 838–840.
- [27] Diederik P. Kingma and Max Welling. 2014. Auto-Encoding Variational Bayes. In 2nd International Conference on Learning Representations, ICLR 2014, Banff, AB, Canada, April 14-16, 2014, Conference Track Proceedings.

- [28] Kezhi Kong, Guohao Li, Mucong Ding, Zuxuan Wu, Chen Zhu, Bernard Ghanem, Gavin Taylor, and Tom Goldstein. 2022. Robust Optimization as Data Augmentation for Large-scale Graphs. In 2022 IEEE/CVF Conference on Computer Vision and Pattern Recognition (CVPR). 60–69. https://doi.org/10.1109/CVPR52688. 2022.00016
- [29] David Krueger, Ethan Caballero, Joern-Henrik Jacobsen, Amy Zhang, Jonathan Binas, Dinghuai Zhang, Remi Le Priol, and Aaron Courville. 2021. Out-of-Distribution Generalization via Risk Extrapolation (REx). In Proceedings of the 38th International Conference on Machine Learning (Proceedings of Machine Learning Research, Vol. 139), Marina Meila and Tong Zhang (Eds.). PMLR, 5815-5826.
- [30] Dongha Lee, SeongKu Kang, Hyunjun Ju, Chanyoung Park, and Hwanjo Yu. 2021. Bootstrapping User and Item Representations for One-Class Collaborative Filtering. In Proceedings of the 44th International ACM SIGIR Conference on Research and Development in Information Retrieval (Virtual Event, Canada) (SIGIR '21). Association for Computing Machinery, New York, NY, USA, 317–326. https://doi.org/10.1145/3404835.3462935
- [31] Pengcheng Li, Runze Li, Qing Da, An-Xiang Zeng, and Lijun Zhang. 2020. Improving Multi-Scenario Learning to Rank in E-commerce by Exploiting Task Relationships in the Label Space. In Proceedings of the 29th ACM International Conference on Information & Knowledge Management. 2605–2612.
- [32] Yong Lin, Qing Lian, and Tong Zhang. 2021. An Empirical Study of Invariant Risk Minimization on Deep Models. ICML 2021 Workshop on Uncertainty and Robustness in Deep Learning (2021).
- [33] Jiashuo Liu, Zheyan Shen, Yue He, Xingxuan Zhang, Renzhe Xu, Han Yu, and Peng Cui. 2023. Towards Out-Of-Distribution Generalization: A Survey. arXiv:2108.13624 [cs.LG]
- [34] Xiaofeng Liu, Chaehwa Yoo, Fangxu Xing, Hyejin Oh, Georges El Fakhri, Je-Won Kang, Jonghye Woo, et al. 2022. Deep unsupervised domain adaptation: A review of recent advances and perspectives. <u>APSIPA Transactions on Signal and Information Processing</u> 11, 1 (2022).
- [35] Yinhan Liu, Myle Ott, Naman Goyal, Jingfei Du, Mandar Joshi, Danqi Chen, Omer Levy, Mike Lewis, Luke Zettlemoyer, and Veselin Stoyanov. 2020. Ro{BERT}a: A Robustly Optimized {BERT} Pretraining Approach. https://openreview.net/forum?id=SyxS0T4tvS
- [36] Jiaqi Ma, Zhe Zhao, Xinyang Yi, Jilin Chen, Lichan Hong, and Ed H. Chi. 2018. Modeling Task Relationships in Multi-task Learning with Multi-gate Mixture-of-Experts. In Proceedings of the 24th ACM SIGKDD International Conference on Knowledge Discovery & Data Mining (London, United Kingdom) (KDD '18). Association for Computing Machinery, New York, NY, USA, 1930–1939. https://doi.org/10.1145/3219819.3220007
- [37] Jiaqi Ma, Zhe Zhao, Xinyang Yi, Jilin Chen, Lichan Hong, and Ed H. Chi. 2018. Modeling Task Relationships in Multi-task Learning with Multi-gate Mixture-of-Experts. In Proceedings of the 24th ACM SIGKDD International Conference on Knowledge Discovery & Data Mining (London, United Kingdom) (KDD '18). Association for Computing Machinery, New York, NY, USA, 1930–1939. https://doi.org/10.1145/3219819.3220007
- [38] Xiao Ma, Liqin Zhao, Guan Huang, Zhi Wang, Zelin Hu, Xiaoqiang Zhu, and Kun Gai. 2018. Entire Space Multi-Task Model: An Effective Approach for Estimating Post-Click Conversion Rate. In The 41st International ACM SIGIR Conference on Research & Development in Information Retrieval (Ann Arbor, MI, USA) (SIGIR '18). Association for Computing Machinery, New York, NY, USA, 1137-1140. https://doi.org/10.1145/3209978.3210104
- [39] Xiao Ma, Liqin Zhao, Guan Huang, Zhi Wang, Zelin Hu, Xiaoqiang Zhu, and Kun Gai. 2018. Entire Space Multi-Task Model: An Effective Approach for Estimating Post-Click Conversion Rate. In The 41st International ACM SIGIR Conference on Research & Development in Information Retrieval (Ann Arbor, MI, USA) (SIGIR '18). Association for Computing Machinery, New York, NY, USA, 1137–1140. https://doi.org/10.1145/3209978.3210104
- [40] Maxime Oquab, Timothée Darcet, Théo Moutakanni, Huy Vo, Marc Szafraniec, Vasil Khalidov, Pierre Fernandez, Daniel Haziza, Francisco Massa, Alaaeldin El-Nouby, et al. 2023. Dinov2: Learning robust visual features without supervision. arXiv preprint arXiv:2304.07193 (2023).
- [41] Judea Pearl. 2009. <u>Causality: Models, Reasoning and Inference</u> (2nd ed.). Cambridge University Press, USA.
- [42] Yunchen Pu, Zhe Gan, Ricardo Henao, Xin Yuan, Chunyuan Li, Andrew Stevens, and Lawrence Carin. 2016. Variational autoencoder for deep learning of images, labels and captions. <u>Advances in neural information processing systems</u> 29 (2016).
- [43] Xubin Ren, Lianghao Xia, Yuhao Yang, Wei Wei, Tianle Wang, Xuheng Cai, and Chao Huang. 2024. SSLRec: A Self-Supervised Learning Framework for Recommendation. In Proceedings of the 17th ACM International Conference on Web Search and Data Mining (Merida, Mexico) (WSDM '24). Association for Computing Machinery, New York, NY, USA, 567–575. https://doi.org/10.1145/3616855.363814
- [44] Steffen Rendle, Christoph Freudenthaler, Zeno Gantner, and Lars Schmidt-Thieme. 2009. BPR: Bayesian personalized ranking from implicit feedback. In Proceedings of the Twenty-Fifth Conference on Uncertainty in Artificial

- $\underline{\text{Intelligence}} \ (\text{Montreal, Quebec, Canada}) \ \underline{\text{(UAI '09)}}. \ \text{AUAI Press, Arlington, Virginia, USA, } 452–461.$
- [45] Yu Rong, Wenbing Huang, Tingyang Xu, and Junzhou Huang. 2020. DropEdge: Towards Deep Graph Convolutional Networks on Node Classification. In International Conference on Learning Representations.
- [46] Shiori Sagawa\*, Pang Wei Koh\*, Tatsunori B. Hashimoto, and Percy Liang. 2020. Distributionally Robust Neural Networks. In <u>International Conference</u> on Learning Representations. https://openreview.net/forum?id=ryxGuJrFvS
- [47] Bernhard Schölkopf, Francesco Locatello, Stefan Bauer, Nan Rosemary Ke, Nal Kalchbrenner, Anirudh Goyal, and Yoshua Bengio. 2021. Towards Causal Representation Learning. arXiv:2102.11107 https://arxiv.org/abs/2102.11107
- [48] Yongduo Sui, Qitian Wu, Jiancan Wu, Qing Cui, Longfei Li, JUN ZHOU, Xiang Wang, and Xiangnan He. 2023. Unleashing the Power of Graph Data Augmentation on Covariate Distribution Shift. In <u>Thirty-seventh Conference on Neural Information Processing Systems</u>.
- [49] Fei Sun, Jun Liu, Jian Wu, Changhua Pei, Xiao Lin, Wenwu Ou, and Peng Jiang. 2019. BERT4Rec: Sequential Recommendation with Bidirectional Encoder Representations from Transformer. In Proceedings of the 28th ACM International Conference on Information and Knowledge Management (Beijing, China) (CIKM '19). Association for Computing Machinery, New York, NY, USA, 1441–1450. https://doi.org/10.1145/3357384.3357895
- [50] Chun How Tan, Austin Chan, Malay Haldar, Jie Tang, Xin Liu, Mustafa Abdool, Huiji Gao, Liwei He, and Sanjeev Katariya. 2023. Optimizing Airbnb Search Journey with Multi-task Learning. In Proceedings of the 29th ACM SIGKDD Conference on Knowledge Discovery and Data Mining. 4872–4881.
- [51] Hongyan Tang, Junning Liu, Ming Zhao, and Xudong Gong. 2020. Progressive Layered Extraction (PLE): A Novel Multi-Task Learning (MTL) Model for Personalized Recommendations. In Proceedings of the 14th ACM Conference on Recommender Systems (Virtual Event, Brazil) (RecSys '20). Association for Computing Machinery, New York, NY, USA, 269–278. https://doi.org/10.1145/3383313.3412236
- [52] Hongyan Tang, Junning Liu, Ming Zhao, and Xudong Gong. 2020. Progressive Layered Extraction (PLE): A Novel Multi-Task Learning (MTL) Model for Personalized Recommendations. In Proceedings of the 14th ACM Conference on Recommender Systems (Virtual Event, Brazil) (RecSys '20). Association for Computing Machinery, New York, NY, USA, 269–278. https://doi.org/10.1145/3383313.3412236
- [53] Aaron van den Oord, Yazhe Li, and Oriol Vinyals. 2019. Representation Learning with Contrastive Predictive Coding. arXiv:1807.03748 [cs.LG] https://arxiv.org/ abs/1807.03748
- [54] Riccardo Volpi, Hongseok Namkoong, Ozan Sener, John Duchi, Vittorio Murino, and Silvio Savarese. 2018. Generalizing to unseen domains via adversarial data augmentation. In Proceedings of the 32nd International Conference on Neural Information Processing Systems (Montréal, Canada) (NIPS'18). Curran Associates Inc., Red Hook, NY, USA, 5339–5349.
- [55] Dongbo Xi, Zhen Chen, Peng Yan, Yinger Zhang, Yongchun Zhu, Fuzhen Zhuang, and Yu Chen. 2021. Modeling the Sequential Dependence among Audience Multistep Conversions with Multi-task Learning in Targeted Display Advertising. In Proceedings of the 27th ACM SIGKDD Conference on Knowledge Discovery & Data Mining (Virtual Event, Singapore) (KDD '21). Association for Computing Machinery, New York, NY, USA, 3745–3755. https://doi.org/10.1145/3447548. 3467071
- [56] Dongbo Xi, Zhen Chen, Peng Yan, Yinger Zhang, Yongchun Zhu, Fuzhen Zhuang, and Yu Chen. 2021. Modeling the Sequential Dependence among Audience Multistep Conversions with Multi-task Learning in Targeted Display Advertising. In Proceedings of the 27th ACM SIGKDD Conference on Knowledge Discovery & Data Mining (Virtual Event, Singapore) (KDD '21). Association for Computing Machinery, New York, NY, USA, 3745–3755. https://doi.org/10.1145/3447548. 3467071
- [57] Fen Xia, Tie-Yan Liu, Jue Wang, Wensheng Zhang, and Hang Li. 2008. Listwise approach to learning to rank: theory and algorithm. In Proceedings of the 25th International Conference on Machine Learning (Helsinki, Finland) (ICML '08). Association for Computing Machinery, New York, NY, USA, 1192–1199. https://doi.org/10.1145/1390156.1390306
- [58] Zhenda Xie, Zheng Zhang, Yue Cao, Yutong Lin, Jianmin Bao, Zhuliang Yao, Qi Dai, and Han Hu. 2022. SimMIM: a Simple Framework for Masked Image Modeling. In 2022 IEEE/CVF Conference on Computer Vision and Pattern Recognition (CVPR). 9643–9653. https://doi.org/10.1109/CVPR52688.2022.00943
- [59] Tiansheng Yao, Xinyang Yi, Derek Zhiyuan Cheng, Felix Yu, Ting Chen, Aditya Menon, Lichan Hong, Ed H. Chi, Steve Tjoa, Jieqi (Jay) Kang, and Evan Ettinger. 2021. Self-supervised Learning for Large-scale Item Recommendations (CIKM '21). Association for Computing Machinery, New York, NY, USA, 4321–4330. https://doi.org/10.1145/3459637.3481952
- [60] Chun-Hsiao Yeh, Cheng-Yao Hong, Yen-Chi Hsu, Tyng-Luh Liu, Yubei Chen, and Yann LeCun. 2022. Decoupled Contrastive Learning. In Computer Vision ECCV 2022: 17th European Conference, Tel Aviv, Israel, October 23–27, 2022, Proceedings, Part XXVI (Tel Aviv, Israel). Springer-Verlag, Berlin, Heidelberg, 668–684. https://doi.org/10.1007/978-3-031-19809-0\_38

- [61] Buyun Zhang, Liang Luo, Yuxin Chen, Jade Nie, Xi Liu, Shen Li, Yanli Zhao, Yuchen Hao, Yantao Yao, Ellie Dingqiao Wen, Jongsoo Park, Maxim Naumov, and Wenlin Chen. 2024. Wukong: Towards a Scaling Law for Large-Scale Recommendation. In Proceedings of the 41st International Conference on Machine Learning (Proceedings of Machine Learning Research, Vol. 235). PMLR, 59421–59434
- [62] Hongyi Zhang, Moustapha Cisse, Yann N. Dauphin, and David Lopez-Paz. 2018. mixup: Beyond Empirical Risk Minimization. In <u>International Conference on</u> Learning Representations.
- [63] Kun Zhang, Bernhard Schölkopf, Krikamol Muandet, and Zhikun Wang. 2013. Domain adaptation under target and conditional shift. In Proceedings of the 30th International Conference on International Conference on Machine Learning -Volume 28 (Atlanta, GA, USA) (ICML'13). JMLR.org, III-819-III-827.
- [64] Zhao-Yu Zhang, Xiang-Rong Sheng, Yujing Zhang, Biye Jiang, Shuguang Han, Hongbo Deng, and Bo Zheng. 2022. Towards understanding the overfitting phenomenon of deep click-through rate models. In Proceedings of the 31st ACM international conference on information & knowledge management. 2671– 2680
- [65] Guorui Zhou, Na Mou, Ying Fan, Qi Pi, Weijie Bian, Chang Zhou, Xiaoqiang Zhu, and Kun Gai. 2019. Deep interest evolution network for click-through rate prediction. In <u>Proceedings of the AAAI conference on artificial intelligence</u>, Vol. 33. 5941–5948.
- [66] Guorui Zhou, Xiaoqiang Zhu, Chenru Song, Ying Fan, Han Zhu, Xiao Ma, Yanghui Yan, Junqi Jin, Han Li, and Kun Gai. 2018. Deep interest network for click-through rate prediction. In <a href="Proceedings of the 24th ACM SIGKDD international conference">Proceedings of the 24th ACM SIGKDD international conference on knowledge discovery & data mining. 1059–1068.</a>
- [67] Xin Zhou, Aixin Sun, Yong Liu, Jie Zhang, and Chunyan Miao. 2023. SelfCF: A Simple Framework for Self-supervised Collaborative Filtering. <u>ACM Trans. Recomm. Syst.</u> 1, 2, Article 9 (June 2023), 25 pages. https://doi.org/10.1145/3591469
- [68] Feng Zhu, Mingjie Zhong, Xinxing Yang, Longfei Li, Lu Yu, Tiehua Zhang, Jun Zhou, Chaochao Chen, Fei Wu, Guanfeng Liu, and Yan Wang. 2023. DCMT: A Direct Entire-Space Causal Multi-Task Framework for Post-Click Conversion Estimation. In 2023 IEEE 39th International Conference on Data Engineering (ICDE). IEEE, 3113–3125. https://doi.org/10.1109/ICDE55515.2023.00239

### A Proofs

# A.1 Derivation of the ELBO<sub>TDS</sub> of Eqn. (2)

Proof.

$$\begin{aligned} & \max_{\theta} \mathbb{E}_{(\mathbf{x}_{u}, \mathbf{x}_{i}, \mathbf{y}_{u}, i, s_{u}, s_{i}) \sim p_{T} \mid \mathbf{s}_{u}, s_{i}, \mathbf{y}_{u}, i}} \left[ \log p_{\theta}(\mathbf{x}_{u}, \mathbf{x}_{i}, \mathbf{y}_{u, i} \mid \mathbf{s}_{u}, \mathbf{s}_{i}) \right] \\ & = \max_{\theta, \phi} \mathbb{E}_{(\mathbf{x}_{u}, \mathbf{x}_{i}, \mathbf{y}_{u}, i, s_{u}, s_{i}) \sim p_{T} \mid \mathbf{s}_{u}, s_{i}, \mathbf{y}_{u}, i}} \left[ \log p_{\theta}(\mathbf{x}_{u}, \mathbf{x}_{i}, \mathbf{y}_{u, i} \mid \mathbf{s}_{u}, \mathbf{s}_{i})} \right] \\ & = \max_{\theta, \phi} \mathbb{E}_{(\mathbf{x}_{u}, \mathbf{x}_{i}, \mathbf{y}_{u}, i, s_{u}, s_{i}) \sim p_{T} \mid \mathbf{s}_{u}, s_{i}, \mathbf{y}_{u}, i}} \left[ \mathbb{E}_{\mathbf{z} \sim q_{\phi}(\mathbf{z}_{u}, \mathbf{z}_{i} \mid \mathbf{x}_{u}, \mathbf{x}_{i})} \log p_{\theta}(\mathbf{x}_{u}, \mathbf{x}_{i}, \mathbf{y}_{u, i} \mid \mathbf{s}_{u}, \mathbf{s}_{i}) d\mathbf{z}_{u} d\mathbf{z}_{i} \right] \\ & = \max_{\theta, \phi} \mathbb{E}_{(\mathbf{x}_{u}, \mathbf{x}_{i}, \mathbf{y}_{u}, i, s_{u}, s_{i}) \sim p_{T} \mid \mathbf{s}_{u}, s_{i}, \mathbf{y}_{u}, i}} \left[ \mathbb{E}_{\mathbf{z} \sim q_{\phi}(\mathbf{z}_{u}, \mathbf{z}_{i} \mid \mathbf{x}_{u}, \mathbf{x}_{i})} \left[ \log p_{\theta}(\mathbf{x}_{u}, \mathbf{x}_{i}, \mathbf{y}_{u, i} \mid \mathbf{s}_{u}, \mathbf{s}_{i}) \right] \right] \\ & = \max_{\theta, \phi} \mathbb{E}_{(\mathbf{x}_{u}, \mathbf{x}_{i}, \mathbf{y}_{u}, i, s_{u}, s_{i}) \sim p_{T} \mid \mathbf{s}_{u}, s_{i}, \mathbf{y}_{u}, i}} \left[ \mathbb{E}_{\mathbf{z} \sim q_{\phi}(\mathbf{z}_{u}, \mathbf{z}_{i} \mid \mathbf{x}_{u}, \mathbf{x}_{i})} \left[ \log \frac{p_{\theta}(\mathbf{x}_{u}, \mathbf{x}_{i}, \mathbf{y}_{u, i} \mid \mathbf{s}_{u}, \mathbf{s}_{i}) p_{\theta}(\mathbf{z}_{u}, \mathbf{z}_{i} \mid \mathbf{x}_{u}, \mathbf{x}_{i})}{p_{\theta}(\mathbf{z}_{u}, \mathbf{z}_{i} \mid \mathbf{x}_{u}, \mathbf{x}_{i})} \cdots \frac{q_{\phi}(\mathbf{z}_{u}, \mathbf{z}_{i} \mid \mathbf{x}_{u}, \mathbf{x}_{i})}{q_{\phi}(\mathbf{z}_{u}, \mathbf{z}_{i} \mid \mathbf{x}_{u}, \mathbf{x}_{i})} \cdot \frac{q_{\phi}(\mathbf{z}_{u}, \mathbf{z}_{i} \mid \mathbf{x}_{u}, \mathbf{x}_{i})}{q_{\phi}(\mathbf{z}_{u}, \mathbf{z}_{i} \mid \mathbf{x}_{u}, \mathbf{x}_{i})} \right] \\ & = \max_{\theta, \phi} \mathbb{E}_{(\mathbf{x}_{u}, \mathbf{x}_{i}, \mathbf{y}_{u}, i, \mathbf{s}_{u}, \mathbf{s}_{i}) \sim p_{T} \mid \mathbf{s}_{u}, \mathbf{s}_{i}, \mathbf{y}_{u}, i}} \mathbb{E}_{\mathbf{z} \sim q_{\phi}(\mathbf{z}_{u}, \mathbf{z}_{i} \mid \mathbf{x}_{u}, \mathbf{x}_{i})} \left[ \log \frac{p_{\theta}(\mathbf{x}_{u} \mid \mathbf{z}_{u}) p_{\theta}(\mathbf{x}_{i} \mid \mathbf{z}_{i}) p_{\theta}(\mathbf{y}_{u}, i \mid \mathbf{z}_{u}, \mathbf{z}_{i}) p_{\theta}(\mathbf{z}_{u} \mid \mathbf{z}_{u}, \mathbf{x}_{i})}{q_{\phi}(\mathbf{z}_{u}, \mathbf{z}_{i} \mid \mathbf{x}_{u}, \mathbf{x}_{i})} \right] \\ & = \max_{\theta, \phi} \mathbb{E}_{(\mathbf{x}_{u}, \mathbf{x}_{i}, \mathbf{y}_{u}, i, \mathbf{s}_{u}, \mathbf{s}_{i}) \sim p_{T} \mid \mathbf{x}_{u}, \mathbf{x}_{i}, \mathbf{y}_{u}, i, \mathbf{x}_{u}, \mathbf{y}_{u}, i} \right] \mathbb{E}_{\mathbf{z} \sim q_{\phi}(\mathbf{z}_{u}, \mathbf{z}_{i} \mid \mathbf{x}_{u}, \mathbf{z}_{i})} \left[ \log \frac{p_{\theta}(\mathbf{x}_{u} \mid \mathbf{z}_{u}) p_{\theta}(\mathbf{x}_{i} \mid \mathbf{z}_{u}) p_{\theta}(\mathbf{y}_{$$

# A.2 Proof of Proposition 1

PROPOSITION 2. Given the user and item feature  $\mathbf{x}_u$  and  $\mathbf{x}_i$  with their respective augmented view  $\mathbf{X}_u = \{\mathbf{x}_u, \mathbf{x}_u^{+,0}, \mathbf{x}_u^{-,1}, ..., \mathbf{x}_u^{-,k}\}$  and  $\mathbf{X}_i = \{\mathbf{x}_i, \mathbf{x}_i^{+,0}, \mathbf{x}_i^{-,1}, ..., \mathbf{x}_i^{-,k}\}$  the InfoNCE loss upper bounds the following expression:  $\mathcal{L}_{\text{InfoNCE}}^u + \mathcal{L}_{\text{InfoNCE}}^i \geq -\mathbb{E}_{\mathbf{x}_u, \mathbf{x}_i}[\mathbb{E}_{\mathbf{z}_u, \mathbf{z}_i}[\log p(\mathbf{z}_u|\mathbf{s}_u) + \log p(\mathbf{z}_u|\mathbf{s}_i) - \log p(\mathbf{z}_u) - \log p(\mathbf{z}_i)]] - c$  where  $c = 2 \log k$ .

PROOF. We prove the proposition by first proving the upper bound of a single InfoNCE, then we combine the the two InfoNCE terms for user- and item-side. We first derive the single InfoNCE loss, following a formulation similar to [53]. Formally, for a feature  $\mathbf{x}$  with their respective augmented view  $\mathbf{X} = \{\mathbf{x}, \mathbf{x}^{+,0}, \mathbf{x}^{-,1}, ..., \mathbf{x}^{-,k}\}$ , where  $\{\mathbf{x}, \mathbf{x}^{+,0}\}$  denotes the positive pair and  $\{\mathbf{x}, \mathbf{x}^{-,l}\}_{l=1}^k$  denotes the negative pairs. With a mild abuse of notation, we leverage  $[\mathbf{y} = \mathbf{0}]$  to indicate the covariate  $\mathbf{x}$  being "positive", and the InfoNCE is dirived as follows.

$$\begin{split} \mathbb{E}_{\mathbf{X}}[\log p(\mathbf{y}=\mathbf{0}|\mathbf{X})] &= \mathbb{E}_{\mathbf{X}}[\log \mathbb{E}_{\mathbf{Z} \sim q(\mathbf{Z}|\mathbf{X})}[p(\mathbf{y}=\mathbf{0}|\mathbf{Z})]] \\ &\geq \mathbb{E}_{\mathbf{X}}[\mathbb{E}_{\mathbf{Z} \sim q(\mathbf{Z}|\mathbf{X})}[\log p(\mathbf{y}=\mathbf{0}|\mathbf{Z})]] \quad (\text{Jensen's inequality}) \\ &= \mathbb{E}_{\mathbf{X}}[\mathbb{E}_{\mathbf{Z} \sim q(\mathbf{Z}|\mathbf{X})}[\log \frac{p(\mathbf{Z}^{+,-}|\mathbf{z},\mathbf{y}=\mathbf{0})p(\mathbf{y}=\mathbf{0})}{\sum_{l=0}^{k} p(\mathbf{Z}^{+,-}|\mathbf{z},\mathbf{y}=l)p(\mathbf{y}=l)}]] \quad (\text{Bayes' rule}) \\ &= \mathbb{E}_{\mathbf{X}}[\mathbb{E}_{\mathbf{Z} \sim q(\mathbf{Z}|\mathbf{X})}[\log \frac{p(\mathbf{z}^{+,0}|\mathbf{z})\prod_{r\neq 0}p(\mathbf{z}^{\mathbf{r}})}{\sum_{l=0}^{k} p(\mathbf{z}^{l}|\mathbf{z})\prod_{r\neq l}p(\mathbf{z}^{\mathbf{r}})}]] \quad (p(\mathbf{y}=l) = \frac{1}{k+1}, \forall l \text{ and independence}) \\ &= \mathbb{E}_{\mathbf{X}}[\mathbb{E}_{\mathbf{Z} \sim q(\mathbf{Z}|\mathbf{X})}[\log \frac{p(\mathbf{z}^{+,0}|\mathbf{z})/p(\mathbf{z}^{+,0})}{\sum_{l=0}^{k} p(\mathbf{z}^{l}|\mathbf{z})p(\mathbf{z}^{l})}]] \quad (\text{divide by } \prod_{r=0}^{k} p(\mathbf{z}^{\mathbf{r}})), \end{split}$$

then we end the proof of InfoNCE by parameterizing via similarity functions:

$$\mathcal{L}_{\text{InfoNCE}} = -\mathbb{E}_{\mathbf{X}} [\mathbb{E}_{\mathbf{Z} \sim q(\mathbf{Z}|\mathbf{X})} [\log \frac{\exp(\text{sim}(\mathbf{z}^{+,0}, \mathbf{z}))}{\sum_{l=0}^{k} \exp(\text{sim}(\mathbf{z}^{l}, \mathbf{z}))}]]$$

We next prove the upper bound of InfoNCE as similar in [2]:

$$\begin{split} \mathcal{L}_{InfoNCE} &= -\mathbb{E}_{\mathbf{X}} \big[ \mathbb{E}_{\mathbf{Z} \sim q(\mathbf{Z}|\mathbf{X})} \big[ \log \frac{p(\mathbf{z}^{+,0},\mathbf{z})/p(\mathbf{z}^{+,0})}{\sum_{l=0}^{k} p(\mathbf{z}^{l},\mathbf{z}) \; p(\mathbf{z}^{l})} \big] \quad \text{(multiply by } p(\mathbf{z}) \big) \\ &= -\mathbb{E}_{\mathbf{X}} \big[ \mathbb{E}_{\mathbf{Z} \sim q(\mathbf{Z}|\mathbf{X})} \big[ \log p(\mathbf{z}|\mathbf{z}^{+,0}) - \log(p(\mathbf{z}|\mathbf{z}^{+,0}) + \sum_{l=1}^{k} p(\mathbf{z}|\mathbf{z}^{-,l})) \big] \big] \\ &= \mathbb{E}_{\mathbf{X}} \big[ \mathbb{E}_{\mathbf{Z} \sim q(\mathbf{Z}|\mathbf{X})} \big[ \log(1 + \sum_{l=1}^{k} \frac{p(\mathbf{z}|\mathbf{z}^{-,l})}{p(\mathbf{z}|\mathbf{z}^{+,0})} \big) \big] \big] \\ &\approx \mathbb{E}_{\mathbf{x}} \big[ \mathbb{E}_{\mathbf{z} \sim q(\mathbf{z}|\mathbf{x})} \big[ \log(1 + k \mathbb{E}_{\mathbf{x}^{+,-}} \big[ \mathbb{E}_{\mathbf{z}^{+,-} \sim q(\mathbf{z}^{+,-}|\mathbf{x}^{+,-})} \big[ \frac{p(\mathbf{z}|\mathbf{z}^{-})}{p(\mathbf{z}|\mathbf{z}^{+,0})} \big] \big] \big] \big] \\ &= \mathbb{E}_{\mathbf{x}} \big[ \mathbb{E}_{\mathbf{z} \sim q(\mathbf{z}|\mathbf{x})} \big[ \log k \frac{p(\mathbf{z})}{p(\mathbf{z}|\mathbf{z}^{+,0})} \big] \big] \\ &= -\mathbb{E}_{\mathbf{x}} \big[ \mathbb{E}_{\mathbf{z} \sim q(\mathbf{z}|\mathbf{x})} \big[ \log \frac{p(\mathbf{z},\mathbf{z}^{+,0})}{p(\mathbf{z})p(\mathbf{z}^{+,0})} \big] \big] - \log k \\ &= -\mathbb{E}_{\mathbf{x} \sim p_{T|\mathbf{x},\mathbf{y}}} \big[ \mathbb{E}_{\mathbf{z} \sim q(\mathbf{z}|\mathbf{x})} \big[ \log p(\mathbf{z}|\mathbf{s}) - \log p(\mathbf{z}) \big] \big] - \log k \quad \text{(alter the notation to align with ELBO)}. \end{split}$$

The last step is to combine the InfoNCE for both user u and item i:

$$\mathcal{L}_{\text{InfoNCE}}^{u} + \mathcal{L}_{\text{InfoNCE}}^{i} \geq -\mathbb{E}_{\mathbf{x}_{u}} \left[ \mathbb{E}_{\mathbf{z}_{u} \sim q(\mathbf{z}_{u}|\mathbf{x}_{u})} \left[ \log p(\mathbf{z}_{u}|\mathbf{s}_{u}) - \log p(\mathbf{z}_{u}) \right] \right] - \mathbb{E}_{\mathbf{x}_{i}} \left[ \mathbb{E}_{\mathbf{z}_{i} \sim q(\mathbf{z}_{i}|\mathbf{x}_{i})} \left[ \log p(\mathbf{z}_{i}|\mathbf{s}_{i}) - \log p(\mathbf{z}_{i}) \right] \right] - 2\log k$$

$$= -\mathbb{E}_{\mathbf{x}_{u},\mathbf{x}_{i}} \left[ \mathbb{E}_{\mathbf{z}_{u},\mathbf{z}_{i}} \left[ \log p(\mathbf{z}_{u}|\mathbf{s}_{u}) + \log p(\mathbf{z}_{u}|\mathbf{s}_{i}) - \log p(\mathbf{z}_{u}) - \log p(\mathbf{z}_{i}) \right] \right] - 2\log k.$$

Now we end the proof.

## **A.3 Proof of Eqn.** (3)

PROOF. We omit the user and item notation here for simplicity, when we assume  $p(\mathbf{z}|\mathbf{s}) \sim N(\mu, \sigma^2)$  for a fix  $\sigma$ , given J augmented views with their respective latent representations  $\{\mathbf{z}^j\}_{j=1}^J$  we have:

$$\begin{split} &p(\mathbf{z}|\mathbf{s}) \propto \prod_{j=1}^{J} \exp\{-\frac{1}{2\sigma^2}(\mathbf{z}^j - \mu)^2\} \\ &= \exp\{-\frac{1}{2\sigma^2} \sum_{j=1}^{J} (\mathbf{z}^j)^2 - 2(\sum_{j=1}^{J} \mathbf{z}^j) \mu + J \mu^2)\} \\ &= \exp\{-\frac{1}{2\sigma^2} (\sum_{j=1}^{J} (\mathbf{z}^j)^2 - 2(\sum_{j=1}^{J} \mathbf{z}^j) \mu + J \mu^2)\} \\ &= \exp\{-\frac{1}{2\sigma^2} (\mu - \frac{1}{J} \sum_{j=1}^{J} \mathbf{z}^j)^2\} \exp\{-\frac{1}{2\sigma^2} (\sum_{j=1}^{J} (\mathbf{z}^j)^2 - \frac{1}{J} (\sum_{j=1}^{J} \mathbf{z}^j)^2)\} \\ &\propto \exp\{-\frac{1}{2\sigma^2} (\sum_{j=1}^{J} (\mathbf{z}^j)^2 - \frac{1}{J} (\sum_{j=1}^{J} \mathbf{z}^j)^2)\} \\ &= \exp\{-\frac{1}{2\sigma^2} (\sum_{j=1}^{J} (\mathbf{z}^j)^2 - 2(\sum_{j=1}^{J} \mathbf{z}^j) \overline{\mathbf{z}} + \sum_{j=1}^{J} \overline{\mathbf{z}}^2)\} \\ &= \exp\{-\frac{1}{2\sigma^2} \sum_{j=1}^{J} ((\mathbf{z}^j)^2 - \mathbf{z}^j \overline{\mathbf{z}} + \overline{\mathbf{z}}^2)\} = \exp\{-\frac{1}{2\sigma^2} \sum_{j=1}^{J} (\mathbf{z}^j - \overline{\mathbf{z}})^2\} \end{split}$$

Dataset	#Users	#Items	#User Feat	#Item Feat	Positive Rate (%)	Split	Total
			total:30	63	is like/is follow	train	5.3M
Kuairand-1K 1K		2.4M	statistical: 0	statistical: 52	1.9/0.1	val	0.7M
			categorical:30	categorical: 11	1.9/0.1	test	0.7M
			total:101	total:105		train	0.7B
Shopee-Small	6.1M	56M	statistical: 59	statistical: 93	Click/Add to Cart/Purchase	val	60M
Shopee-Sman	0.11/1	30101	sequential: 35	sequential: 1	l: 1 14.4/1.4/0.4	test	60M
			categorical: 7	categorical: 11			
			total:101	total:105		train	28B
Shopee-Main	,	,	statistical: 59	statistical: 93	Click/Add to Cart/Purchase	val	0.9B
Shopee-Main	/	/	sequential: 35	sequential: 1	11/1/0.2	test	0.9B

categorical: 11

categorical: 7

Table 4: Statistics of datasets.

# **B** Detailed Experiment Setup

## **B.1** Dataset Selection

Industrial recommender systems leverage large-amount, well-engineered features to enhance prediction accuracy. However, most public datasets are not well-suited for studying Temporal Distribution Shift (TDS) due to their limited feature diversity and lack of temporal granularity. For instance: Ali-CCP[38] and MovieLens[21] contain only a single feature type and a restricted number of features; AE [31] provides sufficient feature complexity but lacks timestamps for samples. After an extensive search, we identify KuaiRand-1K as the most suitable public dataset for studying TDS.

Shopee-Main and Shopee-Small. Shopee-Main is a large-scale dataset collected from 40 days of real traffic logs on Shopee, a leading e-commerce platform. It contains rich feature complexity, making it an ideal benchmark for industrial-scale recommendation tasks. However, due to its size and proprietary nature, it cannot be publicly disclosed. To support future research, we provide Shopee-Small, a curated subset containing 13 consecutive days of data from a smaller region. Both datasets are structured into user sessions, where each session includes a list of items the user has interacted with. We follow the curation strategy from [13], which has been shown to improve model generalization to unseen items.

**Kuairand-1K.** KuaiRand is a video recommendation dataset from the Kuaishou app, available in multiple versions with different data curation strategies. Some versions are heavily curated, removing key temporal distribution shifts (TDS) and making them unsuitable for studying evolving user behavior. Among them, KuaiRand-1K is the only version that explicitly exhibits TDS while maintaining a manageable dataset size, making it a suitable benchmark for evaluating models designed to handle temporal shifts.

**Feature Processing.** For all Shopee and KuaiRand-1K datasets, statistical features are converted into categorical features via bucketization, ensuring consistency across varying feature distributions. Categorical features are processed using embedding lookup tables, which transform discrete values into dense vector representations for model training. All sequential features are also sequences of categorical features (historical purchased item IDs), and are processed with shared embedding lookup tables.

The statistics of the three datasets is given in Table 4. We only count the number of parameters of DNN, which varies with different architectures. The number of parameters in the embedding table is not listed because all methods use the same configuration of a shared embedding table.

#### **B.2** Model Architecture

B.2.1 Offline Evaluation. We employ a twin-tower architecture, where user and item representations are learned separately and combined via a dot product to generate final predictions. A shared embedding layer is used to convert one-hot categorical features into dense embeddings. For model backbone, we use a Multi-Layer Perceptron (MLP) as the primary deep learning architecture for both KuaiRand-1K and Shopee datasets. The detailed model configurations for each dataset are provided in Table 5.

For self-supervised learning (SSL) approaches, including SSL4Rec, SSL4Rec\*, Dino4Rec, and ELBO<sub>TDS</sub>, we introduce a linear encoder after the embedding layer to extract latent representations, ensuring effective feature learning while preserving essential temporal characteristics.

*B.2.2 Online A/B Experiment.* Shopee employs a cascade ranking system, where deploying ELBO<sub>TDS</sub> in only one stage would limit its overall impact. To maximize its effectiveness, we integrate ELBO<sub>TDS</sub> into two key ranking stages: coarse ranking and ranking.

Coarse Ranking Stage: This stage performs a unified ranking on items retrieved from multiple recall (matching) strategies, such as vector-based semantic retrieval and text-based retrieval. The candidate pool is reduced from millions to thousands of items. At this stage, only user-side and item-side features can be used, as item embeddings are precomputed offline and stored in a vector database.

Ranking Stage: In this stage, the candidate set is further refined from thousands to hundreds of items. Unlike coarse ranking, this stage allows for the incorporation of user-item cross features to enhance ranking precision. Additionally, more complex model architectures can

Dataset	methods	Backbone	DNN input dim	DNN	#DNN params
Kuairand single-task	ERM, IRM, V-REx, RVP	MLP	1,488	(128,64,32)	210,944
	SSL4Rec, SSL4Rec*, ELBO <sub>TDS</sub>	MLP	1,488	Encoder(128)+(128,64,32)	243,712
	Dino4Rec,	MLP	1,488	2*Encoder(128)+(128,64,32)	434,176
Kuairand multi-task	ERM, IRM, V-REx, RVP	MLP	1,488	2*(128,64,32)	421,888
	SSL4Rec, SSL4Rec*, ELBO <sub>TDS</sub>	MLP	1,488	Encoder(128)+2*(128,64,32)	296,960
	Dino4Rec,	MLP	1,488	2*Encoder(128)+2*(128,64,32)	487,424
Shopee	ERM, IRM, V-REx, RVP	MLP	3,502	3*(256,128,16)	2,898,432
	SSL4Rec, SSL4Rec*, ELBO <sub>TDS</sub>	MLP	3,502	Encoder(512)+3*(256,128,16)	2,788,352
	Dino4Rec	MLP	3,502	2*Encoder(512)+3*(256,128,16)	4,581,376

Table 5: Model architectures for Kuairand and Shopee.

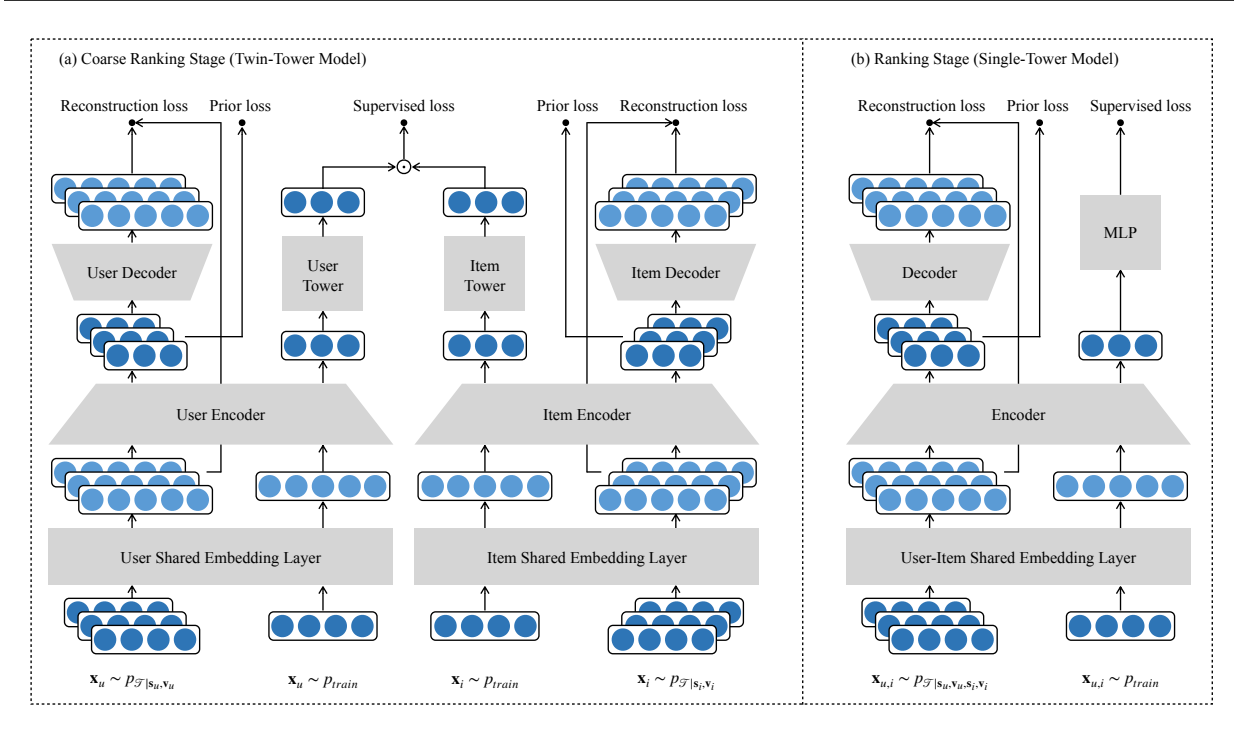


Figure 7: Model architectures on Coarse Ranking Stage and Ranking Stage.

be deployed, replacing the simple dot-product scoring with higher-capacity predictive models, as this stage is allocated more computational resources and latency.

The overall deployment architecture of ELBO<sub>TDS</sub> across these two ranking stages is illustrated in Figure 7.

### B.3 Algorithm

We summarize the detailed implementation of  $ELBO_{TDS}$  in Algorithm 1.

# **B.4** Hyperparameter Details

# Algorithm 1 ELBO<sub>TDS</sub> Training Algorithm

```
Required: training data \{x_u^{(i)}, x_i^{(i)}, y_{u,i}^{(i)}\}_{i=1}^N, batch size B, number of augmentation views J.
    1: for randomly sampled mini-batch \{x_u^{(i)}, x_i^{(i)}, y_{u,i}^{(i)}\}_{i=1}^B do
                      \{\boldsymbol{x}_u^{(i,j)}, \boldsymbol{x}_i^{(i,j)}\}_{i=1}^J \leftarrow \mathcal{T}(\boldsymbol{x}_u^{(i)}, \boldsymbol{x}_i^{(i)}) # augment J views
     2:
     3:
     4:
                      # self-supervised part
                      for j = 1, 2..., J do
     5:
                                 # we fix the variance by 1 in our implementation
     6:
                               # we fix the variance by 1 in our implement \mu_u^{(i,j)}, \sigma_u^{(i,j)} \leftarrow f_{\phi_u}(x_u^{(i,j)})
\mu_i^{(i,j)}, \sigma_i^{(i,j)} \leftarrow f_{\phi_i}(x_i^{(i,j)})
# sample by reparameterization trick
z_u^{(i,j)} \leftarrow \mu_u^{(i,j)} + \sigma_u^{(i,j)} \epsilon_u \quad \epsilon_u \sim \mathcal{N}(0,1)
z_i^{(i,j)} \leftarrow \mu_i^{(i,j)} + \sigma_i^{(i,j)} \epsilon_i \quad \epsilon_i \sim \mathcal{N}(0,1)
# reconstruction
     7:
     8:
     9:
  10:
  11:
                                 \begin{aligned} & \text{\# reconstruction} \\ & \hat{\pmb{x}}_u^{(i,j)} \leftarrow f_{\theta_u}(\pmb{z}_u^{(i,j)}) \text{ and } \hat{\pmb{x}}_i^{(i,j)} \leftarrow f_{\theta_i}(\pmb{z}_i^{(i,j)}) \end{aligned} 
  12:
  13:
  14:
  15:
  16:
                      # supervised part
                      \begin{array}{l} \boldsymbol{\mu}_{u}^{(i)}, \_ \leftarrow f_{\phi_{u}}(\boldsymbol{x}_{u}^{(i)}) \text{ and } \boldsymbol{\mu}_{i}^{(i)}, \_ \leftarrow f_{\phi_{i}}(\boldsymbol{x}_{i}^{(i)}) \\ \hat{\boldsymbol{y}}_{u,i}^{(i)} \leftarrow f_{\theta_{i,l}}(\boldsymbol{\mu}_{u}^{(i)}, \boldsymbol{\mu}_{i}^{(i)}) \end{array}
  17:
  18:
  19:
                      Compute the overall loss \mathcal{L} as in Eqn. (7)
  20:
                      Minimize \mathcal{L} w.r.t. (\phi_u, \phi_i, \theta_u, \theta_i, \theta_{u,i})
  21:
  22: end for
 23: return (\phi_u, \phi_i, \theta_u, \theta_i, \theta_{u,i})
```

Table 6: Hyper-parameters of ELBO<sub>TDS</sub>.

	Optimizer	lr	α	р	r	$p_{seq}$	$p_{cate}$	J
Kuairand single-task	Adam	0.0003	5.0	0.2	2	0.2	0.2	4
Kuairand multi-task	Adam	0.0003	10.0	0.2	2	0.2	0.2	4
Shopee	Adam	0.0005	0.001	0.2	2	0.2	0.2	4

dropout rate for sequential feature  $p_{seq} \in \{0.1, 0.2, 0.3\}$ , embedding dropout rate for categorical feature  $p_{cate} \in \{0.1, 0.2, 0.3\}$ , number of augmentation views  $J \in \{2, 3, 4\}$ . The hyper-parameters are summarized in Table 6.

#### **B.5** Hardware and Software

We conduct our experiment for Kuairand on NVIDIA V100 (16 GB GPU) machine with PyTorch, and experiment for Shopee on NVIDIA A30 (24 GB GPU) machine with Tensorflow.

# **B.6** Additional Online Results

To further analyze the impact of ELBO<sub>TDS</sub>, we conducted a post-launch ablation study to assess its contribution at each ranking stage:

Deploying ELBO<sub>TDS</sub> in the coarse ranking stage alone resulted in a 0.6% uplift in GMV per user. Deploying ELBO<sub>TDS</sub> in the ranking stage alone led to a 2% uplift in GMV per user. Deploying ELBO<sub>TDS</sub> in both stages simultaneously yielded a combined uplift slightly lower than the

alone led to a 2% uplift in GMV per user. Deploying ELBO $_{TDS}$  in both stages simultaneously yielded a combined uplift slightly lower than the sum of individual improvements, due to the complex system dynamics. The smaller impact of coarse ranking is expected, as it is farther from direct user interactions. Additionally, the re-ranking stage, which operates above the ranking stage, introduces further adjustments that influence the final performance of ELBO $_{TDS}$ .

# B.7 More details of our Empirical Observation

In this section, we provide an in-depth analysis of temporal distribution shifts affecting three feature types in Shopee: **statistical features**, **sequential features**, **categorical features**.

	Train (ms)	Infer (ms)
ERM	995	204
ELBO <sub>TDS</sub> (#aug=1)	999	190
ELBO <sub>TDS</sub> (#aug=2)	1122	192
ELBO <sub>TDS</sub> (#aug=3)	1262	198
$ELBO_{TDS}(\#aug=4)$	1611	207

Table 7: Training and inference time per batch on Shopee-Small dataset.

**1. Statistical Features** are aggregated metrics that reflect user-item interaction trends over time, such as click-through rate (CTR) or conversion rate (CTCVR) over the past 3 days. To quantify their fluctuation intensity, we compute the coefficient of variation (CV), defined as:  $CV(f_i) = std(f_i)/mean(f_i)$ , where a higher CV value indicates greater temporal variation.

As shown in Figure 2 (a), 3-day mean CTR and 3-day mean CTCVR exhibit CV values around 3-5, suggesting significant temporal shifts in  $p(\mathbf{x}_{stat}|\mathbf{x}_{cate})$ . Here, the distribution of statistical features is conditioned on categorical features, as statistical features are typically aggregated over specific category values (e.g., CTR per item ID).

2. Sequential Features represent user or item behavior histories, such as a user's purchased item IDs over the past 30 days. To analyze their temporal shifts, we apply FP-Growth [20], a scalable frequent pattern mining algorithm, to extract co-occurrence patterns within user/item behavior sequences for the same targets. For example, if a user purchases item A today, they may have also purchased items B and C in the past 30 days. Understanding these sequential patterns helps quantify how user behavior evolves over time.

Because attention-based models are widely used in sequential recommendation [65, 66], the matched frequent item set can be viewed as a subset of highly relevant items which an attention model might capture. We measure fluctuation intensity of the frequently matched set's size using CV over a 30-day period (Figure 2 (b)). The results indicate mild turbulence, with most CV values around 0.4, confirming a temporal shift in  $p(\mathbf{x}_{seq}|\mathbf{x}_{cate})$ . Similar to statistical features, sequential feature distributions are also conditioned on categorical features (e.g., user purchasing history w.r.t. user ID or item sale history w.r.t. item ID).

**3. Categorical Features** represent semantic attributes such as user demographics and product categories. To quantify their temporal variation, we compute the Jensen-Shannon Divergence (JSD) to measure feature value distribution shifts: Between adjacent days and Between the first day and each subsequent day. Figure 2 (c) shows that categorical features exhibit notable day-to-day distribution shifts, with an increasing cumulative divergence over time, indicating a temporal shift in  $p(\mathbf{x}_{cate})$ .

**Overall**, the temporal shifts in each feature type contribute to the overall joint distribution shift through the following factorization:  $p(\mathbf{x}_{stat}, \mathbf{x}_{seq}, \mathbf{x}_{cate}) = p(\mathbf{x}_{stat}|\mathbf{x}_{cate})p(\mathbf{x}_{seq}|\mathbf{x}_{cate})p(\mathbf{x}_{cate})$ , where we assume  $\mathbf{x}_{stat} \perp \mathbf{x}_{seq}|\mathbf{x}_{cate}$  (i.e., statistical and sequential features are conditionally independent to each other given categorical features). This decomposition highlights how temporal drifts in different feature types collectively induce shifts in the overall data distribution.

Notably, Figure 2 (c) reveals a cumulative yet gradual shift over time, aligning with our intuition. For instance, children's product preferences differ significantly from adults', and popular trends evolve year by year. This observation supports our focus on TDS within a manageable time window, where short-term user preferences remain relatively stable despite ongoing shifts. Within this window, time-varying factors act more like noisy fluctuations, interfering with the model's ability to capture consistent user intent and short-term behavioral patterns. To accommodate long-term changes, we currently employ incremental training with ELBO<sub>TDS</sub>, allowing the model to adapt dynamically while mitigating the impact of temporal fluctuations. Addressing broader, lifelong learning challenges in recommender systems remains an open research direction for future exploration.

## C Additional Experimental Results

# C.1 Model Efficiency

We evaluate the per-batch training and inference time of ELBO<sub>TDS</sub> on the Shopee-Small dataset using our internal training platform (Table 7). During training, the augmentation incurs only minimal overhead, as augmented views are passed through lightweight encoder and decoder components, bypassing the heavy multi-task backbone. At inference time, ELBO<sub>TDS</sub> behaves almost identically to ERM, introducing no additional computational burden. Notably, our method has been successfully deployed in Shopee Search without requiring additional storage for training samples.

#### C.2 Result on MMoE backbone

To further assess the effectiveness of ELBO $_{TDS}$ , we conduct extensive experiments using an advanced multi-task learning backbone, MMoE [37], on both the Shopee-Small and Kuairand-1K datasets. The AUC and GAUC results are reported in Tables 8 and 9. Across both datasets, ELBO $_{TDS}$  consistently achieves the highest AUC and GAUC scores, confirming its effectiveness and generalizability across different backbone architectures.

Table 8: Multi-task listwise ranking on Shopee-Small with MMoE backbone.

backbone: MMoE	Click		Add-t	o-Cart	Purchase	
loss: CE&ListNet[5]	AUC	GAUC	AUC	GAUC	AUC	GAUC
ERM	0.8001	0.7919	0.8496	0.7982	0.8895	0.8204
IRM	0.7803	0.7734	0.8083	0.7617	0.8430	0.7844
V-REx	0.7833	0.7768	0.8160	0.7716	0.8452	0.7893
RVP	0.7832	0.7763	0.8145	0.7680	0.8427	0.7842
DINO4Rec	0.7973	0.7908	0.8462	0.7940	0.8864	0.8176
SSL4Rec	0.7959	0.7900	0.8465	0.7940	0.8869	0.8159
SSL4Rec*	0.7993	0.7926	0.8475	0.7948	0.8882	0.8194
$ELBO_{TDS}$	0.8036	0.7966	0.8538	0.8015	0.8925	0.8251

Table 9: Single- and multi-task ranking performance on the Kuairand-1K dataset.

	single-task		multi-task				
backbone: MMoE	is_	like	is_	is_like		ollow	
	AUC	GAUC	AUC	GAUC	AUC	GAUC	
ERM	0.9048	0.5031	0.9035	0.4913	0.7913	0.5022	
IRM	0.9036	0.5052	0.9012	0.4924	0.7879	0.5017	
V-REx	0.9055	0.5048	0.9018	0.4925	0.7907	0.5017	
RVP	0.9012	0.5046	0.8999	0.4910	0.7771	0.5031	
Dino4Rec	0.9051	0.5002	0.9043	0.5012	0.7922	0.4967	
SSL4Rec	0.9060	0.4946	0.9066	0.5011	0.7934	0.4950	
SSL4Rec*	0.9061	0.4974	0.9047	0.4937	0.7937	0.4989	
$ELBO_{TDS}$	0.9102	0.5092	0.9084	0.5096	0.8241	0.5041	

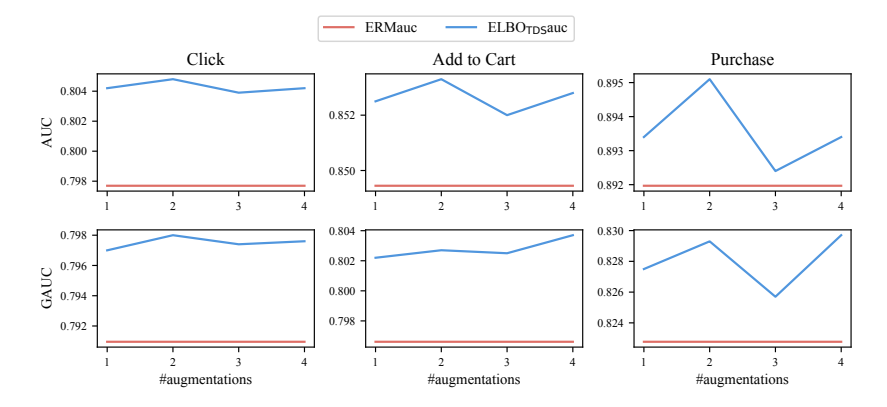


Figure 8: AUC and GAUC w.r.t. #augmentations on Shopee-Small.

## C.3 Sensitivity on #Augmentations

We further investigate the sensitivity of  $ELBO_{TDS}$  to the number of augmented views. Figure 8 presents the AUC and GAUC results on Shopee-Small with varying numbers of augmentations. We observe that model performance remains relatively stable across 1 to 4 augmentations, indicating that  $ELBO_{TDS}$  is robust to this hyperparameter.

## D Relation to Causal Inference

Causal inference seeks to identify the cause and effect between variables, generally via climbing the ladder of causation: 1) association; 2) intervention 3) and counterfactual [41]. Regarding counterfactual reasoning to address TDS, the goal is generalizing to the counterfactual distribution  $p^{cf}(\mathbf{x}, \mathbf{y})$  which is obtained by three steps: 1) (abduction) recovering  $p(\mathbf{z})$ ,  $p(\mathbf{s})$ , and  $p(\mathbf{v})$  from the observation  $p(\mathbf{x}, \mathbf{y})$ ; 2) (action) intervene the time-varying  $p(\mathbf{v})$  to  $p^{cf}(\mathbf{v})$ ; 3) (prediction) obtaining the counterfactual distribution via ancestral sampling on the causal model  $\mathcal{M}$ :  $p^{cf}(\mathbf{x}, \mathbf{y}) = \int p_{\mathcal{M}}(\mathbf{x}, \mathbf{y}|\mathbf{z})p_{\mathcal{M}}(\mathbf{z}|\mathbf{s}, \mathbf{v})p_{\mathcal{M}}(\mathbf{s})p^{cf}(\mathbf{v})d\mathbf{z}d\mathbf{s}d\mathbf{v}$ . Obtaining the causal model  $\mathcal{M}$  requires additional strict data assumptions [41, 47], and a not accurately estimated  $\mathcal{M}$  can risk downgrading the model performance, making it difficult to apply in industrial application.

Instead, our approach can be seen as a non-strict counterfactual reasoning approach, where the ancestral sampling is approximated by our well-designed data augmentation based on the empirical observation, to simulate the time-varying  $p^{cf}(\mathbf{v})$ , and incorporating with our ELBO<sub>TDS</sub> (relaxing the assumption to only the conditional independence embded in the causal graph in Figure 1) to capture robust informative representation despite the time-varying disturbance.

## E Differences between TDS and Covariate Shift/Correlation Shift

Temporal Distribution Shift (TDS) is a specific form of distribution shift that arises when the joint data distribution changes over time. While TDS can be analyzed within the broader framework of General Distribution Shift (GDS), it exhibits several distinguishing characteristics that set it apart from the conventional **covariate shift** and **correlation shift**.

In **covariate shift**, it is typically assumed that the input distribution changes between training and testing, i.e.,  $p_{train}(\mathbf{x}) \neq p_{test}(\mathbf{x})$ , while the conditional distribution remains invariant, i.e.,  $p_{train}(\mathbf{y}|\mathbf{x}) = p_{test}(\mathbf{y}|\mathbf{x})$  [48, 63]. However, this assumption often fails in real-world settings. For instance, in the case of consumer behavior during a promotional event, both the feature distribution e.g., price or context and the conditional distribution e.g., probability of purchase for a luxury item—are impacted simultaneously. As a result, the standard covariate shift assumption does not hold over time in industrial environments that are sensitive to seasonal, promotional, or other periodic events.

Similarly, **correlation shift** is characterized by changes in  $p_{train}(y|\mathbf{x}) \neq p_{test}(y|\mathbf{x})$ , under the assumption that  $p_{train}(\mathbf{x}) = p_{test}(\mathbf{x})$  [48]. In our setting, this assumption is also violated. Promotional and seasonal factors lead to shifts in both user intent and feature distributions, making it difficult to isolate a purely conceptual change.

Overall, these dynamics cannot be fully addressed by methodologies designed solely around either covariate or correlation shift frameworks.

Received 20 February 2007; revised 12 March 2009; accepted 5 June 2009